Bio-based High Performance Polymers from 4-Aminocinnamate Photodimers

by

PHRUETCHIKA SUVANNASARA

Submitted to

Japan Advanced Institute of Science and Technology

In partial fulfillment of the requirements

For the degree of

Doctor of Philosophy

Supervisor: Associate Professor Tatsuo Kaneko

School of Materials Science

Japan Advanced Institute of Science and technology

March 2014

CONTENTS

CHAPTER 1

GENERAL INTRODUCTION

CHAPTER 1
GENERAL INTRODUCTION

1.1 Environmental problems and renewable materials

Diversity of human activities has a vital impact on the environment and has caused numerous problems [1]. Overconsumption of nonrenewable resources that persists for many years has caused environmental problems such as carbon dioxide condensation in the earth's atmosphere which is a serious factor enhancing global warming [2]. One of the main parts of household wastes is plastic which mostly comes from petroleum based polyolefins such as polyethylene, polypropylene, polyvinylchloride, polystyrene, etc. and contributes greatly to environmental and social problems due to the loss of natural resources and the limited amount of petroleum. Therefore, the use of environmentally friendly polymers originating from renewable starting materials and/or degrading in the environment is hugely significant with respect to the reduction of waste. Bio-based polyesters played a predominant role as degradable plastics owing to their potentially hydrolysable ester [3]. However, some aliphatic bio-based polyesters, such as poly(hydroxyalkoate)s [4], poly(butylenes succinate) [5], and so on [6], showed low performance and less functions which were not enough to use as super-engineering plastics. Moreover, these polyesters had become substitutes for only a small amount percentage of the currently used plastic materials. A number of polymers such as Ecoflex^{TM} [7] and Biomax^{TM} [8] were used to improve durability and performance. However, they still had problem due to their toxicity. Polymers that were able to cleave and change to oligomer or monomer, and had a performance closer to that of engineering plastics would be highly desirable for semipermanent carbon stock.

1.2 Carbon stock

Carbon fixation from the atmosphere into biomolecules such as sugars via photosynthesis and the development of durable bioplastics or usage of recyclable bioplastics derived from biomolecules contributes the long term carbon stock. However, the concept of long term carbon stock cannot be achieved by the usage of biofuels and nondurable polymers since they return carbon dioxide back into an atmosphere very quickly and accelerate global warming. The process of achieving net zero of carbon dioxide emission by balancing a measured amount of carbon released from both biofuels and nondurable polymer with an equivalent amount sequestered or offset from photosynthesis and polymer production to make up the difference is called carbon neutrality (Figure 1.1).

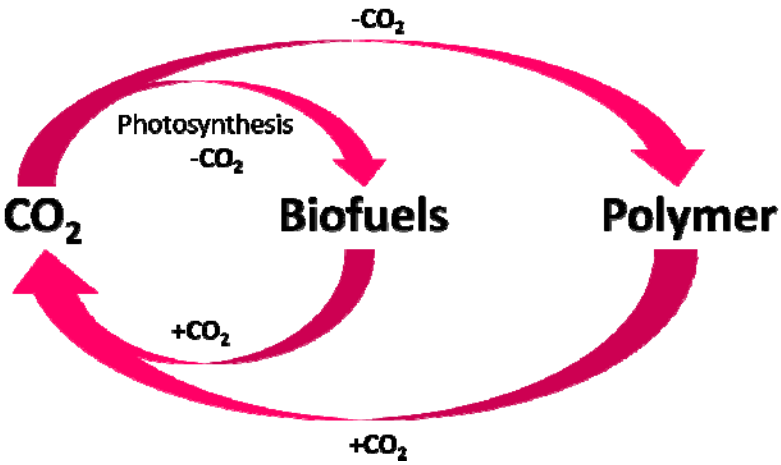

Figure 1.1 Carbon neutrality: balancing an amount of carbon dioxide emission with carbon dioxide consumption.

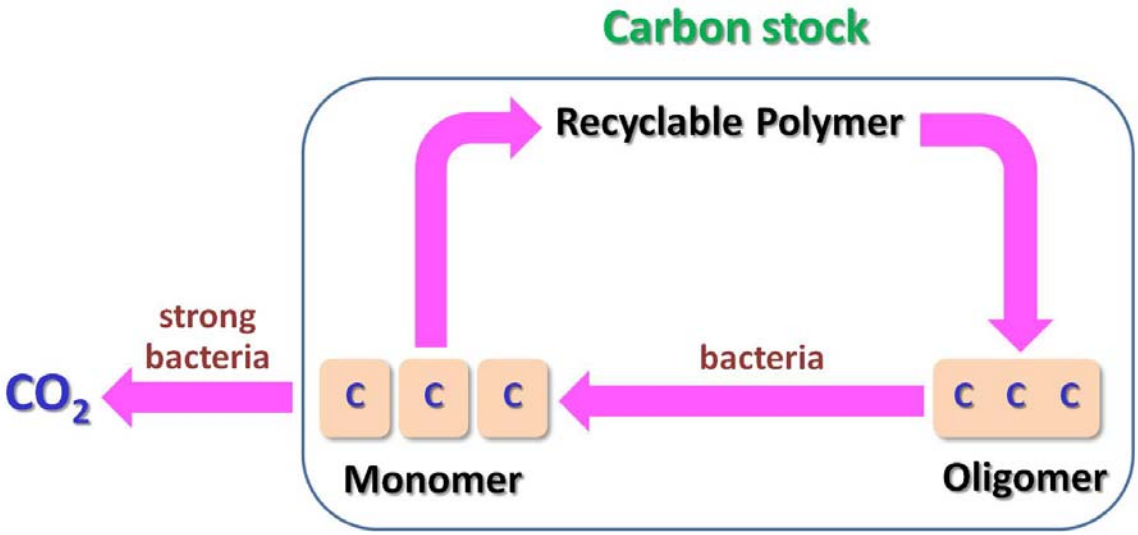

Figure 1.2 The concept of carbon stock in recyclable or durable polymers.

Recyclable plastics which can be used many times prolong carbon in the polymer structure. They are cleaved to become oligomers or monomers by some bacteria and these monomers or oligomers can potentially be used to synthesize polymer again. Carbon fixation in this cycle is maintained as carbon stock due to the durability of materials. In case of nondurable polymers, they would be decomposed by bacteria and then carbon dioxide is released to the atmosphere. Therefore, the concept of carbon stock is indispensable in worldwide societies to help the earth.

1.3 Bio-based monomers

Bio-based monomers play an important role in the syntheses of bio-based polymers and were the main focus in this research. The bio-based monomers which were used in the research are as follows.

1.3.1 Cinnamic acid and Cinnamate derivatives

It is known that many biomonomers exist in plants such as tyrosine, vanillic acid, coumaric acid derivatives, cinnamic acid derivatives and so on. Cinnamic acid is a white crystalline compound with a formula $C_6H_5CHCHCO_2H$ and slightly soluble in water but freely soluble in many organic solvents. It exists as both a *cis* and a *trans* isomer, although the latter is more common.

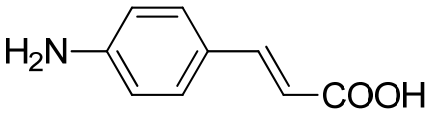

Figure 1.3 The chemical structure of 4ACA.

There are a number of cinnamate derivatives representing aromatic biomolecules in living organisms from photosynthetic bacteria [9] to higher plants [10] such as *p*-coumaric acid (4HCA), *m*-coumaric acid (3HCA), caffeic acid (DHCA), ferulic acid (MHCA) and 4-aminocinnamic acid (4ACA; Figure 1.3). Cinnamates have been used in a photoreactions to produce various chemical materials [11]. Therefore, 4-aminocinnamic acid (4ACA) is an attractive option because the [2+2] photocycloaddition of the cinnamates is one of the most efficient chemical reactions if the reaction condition is well arranged.

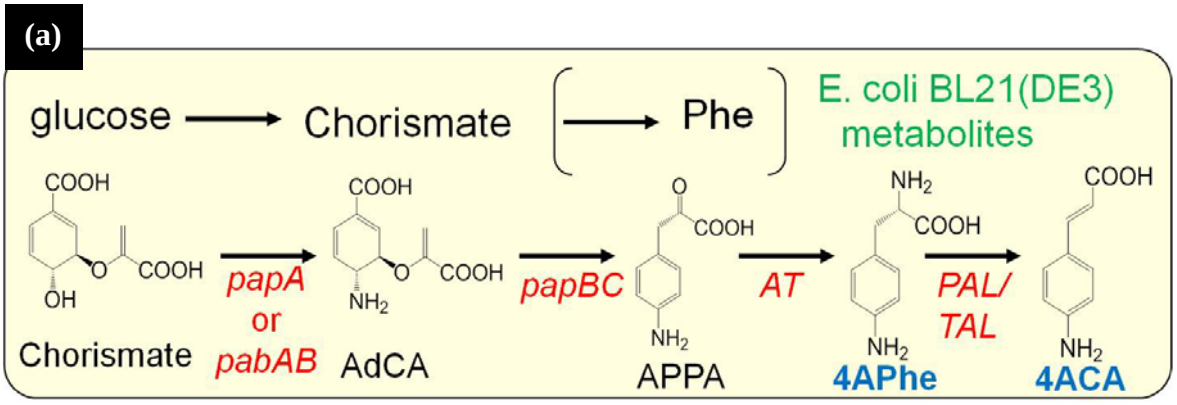

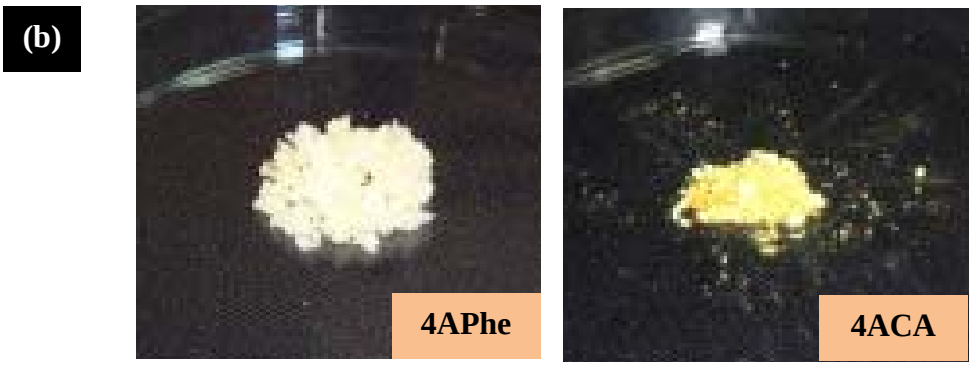

Figure 1.4 (a) 4ACA biosynthesis pathways from 4APhe and (b) physical appearances of 4APhe and 4ACA obtained from biosynthesis.

A report has shown that some bacteria produced 4-aminophenylalanine (4APhe) as an intermediate of antibiotics [12]. There are established systems for fermenting glucose or biomass to produce 4APhe [13, 14]. 4ACA can be obtained from 4APhe under a kind of phenylalanine ammonia lyases, which deaminate α-amino residue of phenylalanine (or its derivatives) to generate cinnamic acid (or its derivatives) (Figure 1.4). However, the bioavailability of 4ACA is unclear. We accordingly investigated the deamination of 4APhe to synthesize biomass-derived 4ACA by using recombinant phenylalanine ammonia lyases. One isozyme, phenylalanine ammonia lyase 4 (AtPal4) of *Arabidopsis thaliana*, was functionally produced in recombinant *Escherichia coli*. The strain produced 1.4 x 10^{-2} and 3.8 x 10^{-4} μmol min^{-1} mg^{-1} of phenylalanine- and 4APhe- ammonia lyase activity, respectively, indicating that AtPal4 used 4APhe as a substrate. Incubating the bacterial cells with 4APhe decreased the amount of 4APhe produced and generated 0.13 g/L of 4ACA (Figure 1.5). This indicated that combination of this process and the 4APhe fermenting system produced 4ACA from the biomass.

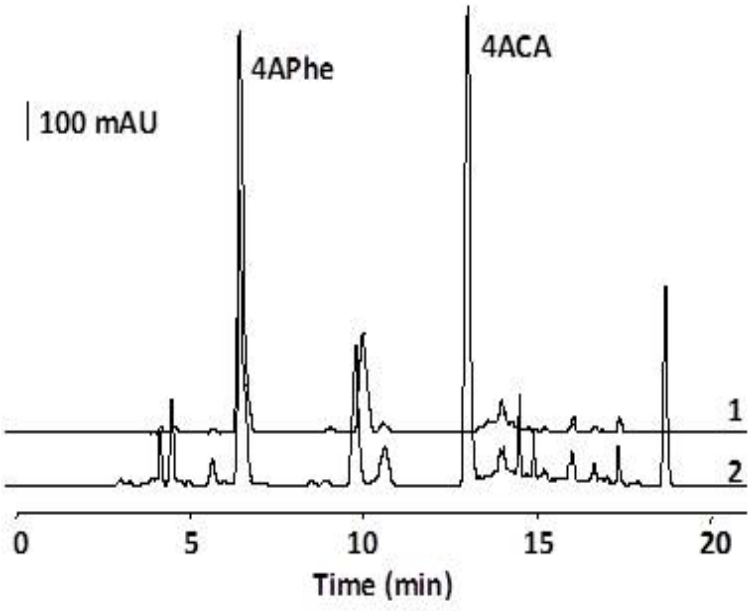

Figure 1.5 High-performance liquid chromatography (HPLC) separation of 4ACA bio-converted from 4APhe. The AtPal4 producing recombinant *E. coli* was incubated with 10 mM 4APhe at 37 °C for 0 hour (line 1) and 12 h (line 2).

1.3.2 Dipicolic acid

Dipicolinic acid (pyridine-2,6-dicarboxylic acid or PDC or DPA; Figure 1.6) is a chemical compound which composes 5% to 15% of the dry weight of bacterial spores [15]. It is implicated as responsible for the heat resistance of the endospore. However, mutants resistant to heat but lacking dipicolinic acid have been isolated, suggesting other mechanisms contributing to heat resistance are at work.

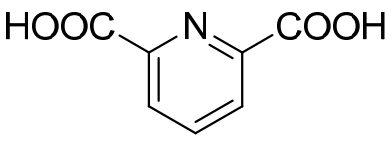

Figure 1.6 The chemical structure of dipicolinic acid.

1.3.3 1,2,3,4-Cyclobutane tetracarboxylic acid dianhydride

1,2,3,4-Cyclobutane tetracarboxylic acid dianhydride (CBDA; Figure 1.7) is a dianhydride compound which is converted from maleic acid dimethyl ester. UV irradiation of maleic acid dimethyl ester and ring closure by acetic anhydride produced CBDA.

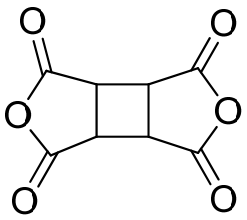

Figure 1.7 The chemical structure of CBDA.

1.4 High performance polymers

High performance polymers exhibit exceptional stability upon exposure to some harsh environmental conditions and have properties that surpass those of traditional polymers. These materials are defined in many ways depending on the application and, to some extent, the organized systems used for developing or employing the materials. They have properties that include outstanding thermal resistance and/or mechanical strength, low specific density, high conductivity, high thermal, electrical, or sound insulation properties or superior flame resistance [16]. The factors that contribute to the high performance and heat resistance properties of these polymers are: resonance stabilization, primary bond strength, molecular symmetry, secondary bonding forces, molecular weight and distribution, rigid intrachain structure, cross-linking, mechanism of bond cleavage and additives or reinforcements (fillers, clays, miscellaneous nanoparticles) [17]. They have been used in many industries ranging from

communication to medicine and to transportation [18]. Because of the superior performance characteristics of high performance polymers, the demand for this type of polymeric materials is growing steadily. Although several applications do not require usage at high temperature, the fabrication process leading to the parts or components requires the polymer to be thermally stable. Here, I focused on two kinds of high performance polymers: polyamide and polyimide.

1.4.1 Polyamide

Polyamides are high molecular weight materials containing intermittent amide units and the hydrocarbon segments that can be aliphatic, partially aromatic, or wholly aromatic. The type of hydrocarbon segment employed has effects on the chain flexibility and structural regularity, with the latter important in the formation of crystalline phase. Polyamides are often called nylons, the trade name given to them by DuPont. Partially aromatic and wholly aromatic polyamides have been successfully developed [19]. They have good mechanical properties due to formation of hydrogen bonds. The hydrogen bond increases the chain interaction resulting in higher yield stress, fracture stress, impact strength, tear strength, and abrasion resistance [16]. Polyamides have been used essentially as fibers, films, and filler-containing engineering plastics for special applications [20]. Most of the reinforced polyamides are filled with glass fibers and to a lesser extent with particles, e.g., talc, kaolin, and mica. For engineering plastics applications, dimensional stability at high temperatures is often sought. Wholly aromatic polyamides can be processed from solution either into films or into fibers. These polymers have very good dimensional stability [16] and excellent heat resistance [21, 22]. Partially aromatic polyamides have higher glass transition and

melting temperatures compared to their aliphatic counterparts. They can be prepared by various methods, e.g., mono-add systems which both acid and amine functionalities are on the same molecule and di-add systems such as diacids, diacid chlorides or diesters in combination with either aromatic or aliphatic diamines, as well as, the reactions between diisocyanates and diacids which are commonly used for this propose. Wholly aromatic polyamides have high glass transition temperature (>200 °C) and, when in the form of crystalline, show very high melting temperature (>500 °C). High-molecular-weight polymers cannot be prepared by melting or melt processing, because many aromatic diacids are decarboxylates and aromatic diamines are readily oxidized and have a tendency to sublime at elevated temperature. Their synthesis is usually carried out in solution and due to the very low solubility, special solvents are required to obtain high-molecular-weight polymers.

1.4.2 Polyimides

It is well known that polyimides (PIs) based on aromatic ring structures not only have excellent thermal property, thermooxidative stability and mechanical strength, but also a relatively low dielectric constant and superior chemical resistance [23, 24, 25]. Hence, PIs have been widely used in many applications such as in the fields of adhesives, composite materials, aerospace, microelectronics, and optoelectronics industries [26, 27]. PIs are often made by a two-step process. First, the poly(amic acid)s (PAAs) are made by reaction of diamines with dianhydride at low temperature in polar solvents. In the second step, PAAs are cured by either thermal or chemical treatment to obtain PIs [28]. Although significant improvements in the performances of PI materials

have been made in recent years [29, 30, 31], the further development of PIs is still required to meet increasing demands and reduce production costs.

The objective of this research was to develop high performance polymers which made up the majority of super-engineering plastics with their excellent thermomechanical properties, superior chemical resistance, and high dielectric breakdown strength from bio-based monomer. Moreover, polymers generally show excellent durability, which means less environmental-degradability, and might sometimes induce the negative effects on the establishment of green-sustainable society. Hence, the polymers with sufficiently-high performance during use but with degradability under specific condition (UV light with a specific wavelength range) are strongly requested.

CHAPTER 2

SYNTHESES AND CHARACTERIZATION OF BIO-BASED AROMATIC DIAMINE AND BIO-BASED POLYAMIDE DERIVED FROM 4-AMINOCINNAMATE BIOCHEMICALS

CHAPTER 2

SYNTHESES AND CHARACTERIZATION OF BIO-BASED AROMATIC DIAMINE AND BIO-BASED POLYAMINE DERIVED FROM 4-AMINOCINNAMATE BIOCHEMICALS

2.1 Introduction

Recently, demand for plastics has increased and plastics played an important role in the modern industrial and commercial applications [1]. The world wide annual production of plastics will surpass 300 million ton in 2010-2015. Today, a large amount of plastics were produced from petrochemicals. However, they currently had serious problems associated with the limited amount of petrochemicals and their long term resistance to degradation by living system resulting in environmental problems. Therefore, development of bio-derived environmentally-benign polymer was extremely interesting because it was able to reduce the amounts petroleum consumption and plastic dust by decomposition by environmental functions such as sun light, rain and biological activity such as microorganism. Material derived from biological resources, such as, DNA, proteins, and other metabolites including cinnamic acid derivative which was used in this research. Cinnamic acid as bioavalible compound could be converted to starting materials to synthesize bio-based monomers and was widely known as photoreactive chemical compounds [32]. These bio-based monomers could be polymerized to create the family of bio-derived polymers. A number of bio-derived polymers such as polyethylene, poly (propylene carbonate), aliphatic polyesters; poly (hydroxyl alkanoate)s [33], poly(butylenes succinate) [33] and poly(lactic acid) [34],

semi-aromatic polyester; poly (ethylene terephthalate) (PET) and poly (trimethylene terephthalate) (PTT), and polyamide. Nevertheless, the applications of bio-derived polyethylene, poly (propylene carbonate) and polyesters are limited due to their low glass transition temperature which was unsuitable for high-temperature processing. I focused on super-engineering plastics, especially polyamides containing aromatic ring because they have high thermal, mechanical, and chemical resistant properties.

Kevlar^{TM} was one of the best aromatic polyamide which is consists of *p*-phenylene diamine and terephthalic acid dichloride. However, aromatic diamine which was used to synthesize Kevlar^{TM} was not derived from living organism.

Here we tried to describe the syntheses of the aromatic diamine monomers from a bio-derived compound, 4-aminocinnamic acid (4ACA), even aromatic diannilines were difficult to derive from bioorganisms due to their toxicity. Light, as a remote stimulus, was an attractive nano-object disassembling driving force, which had been intensively investigated for two obvious advantages: (1) light can be accurately targeted and highly selective; (2) in contrast to chemical stimuli, no acid, bases, or other reagents have to be brought into the system from outside, which in many case could be technically challenging. Therefore, photocycloaddition was used to synthesize 4,4'-diamino-α-truxillic acid dihydrochloride. The single crystallography was used to confirm the stereostructure of new product. Moreover, one kind of bioavalible compounds was dipicolic acid which composed of 5 % to 15 % of dry weight of bacterial spore. It was famous bio-compound containing aromatic diacid structures. Finally, bioavalible 4,4'-diamino-α-truxillic acid derivative and dipicolic acid were used as monomer to polymerize polyamide in next step to reduce the problem of plastics.

2.2 Experimental Section

2.2.1 Materials

4-aminocinamic acid (4ACA) was purchased from TCI. Trimethylsilyl chloride ($(CH_3)_3SiCl$) and triphenyl phosphite ($(PhO)_3P$) were purchased from Aldrich Chemical. Hydrochloric acid (HCl), sodium hydroxide (NaOH), sodium sulfate (Na_2SO_4), pyridine and *N*-Methyl-2-pyrrolidone (NMP, 99 % anhydrous) were purchased from Kanto Chemical and were used as chemical reagent and drying agent. Dipicolic acid was obtained from Nacalai Tesque. All other reagents such as methanol, ethanol, acetone and hexane were obtained from various commercial sources and used as a solvent for reactions.

2.2.2 Characterization

The ^{1}H NMR, ^{13}C NMR, ^{1}H-^{13}C HSQC and ^{1}H-^{13}C HMBC spectra were determined by Bruker Biospin AG 400 MHz, 54 mm spectrometer using DMSO-d_6 as solvent. Melting temperate was recorded with Mettler FP90 Central Processor and Mettler FP82HT Hot stage. FTIR spectra were recorded with Perkin Elmer, Spectrum One. The mass spectra were measured using Fourier transform ion cyclotron resonance mass spectrometer (FT-ICR MS, Solarix), scanned from *m/z* 150 to *m/z* 1000.

2.2.3 Monomer Syntheses

2.2.3.1 Synthesis of 4,4'-diamino-α-truxillic acid dihydrochloride 12 N Hydrochloric acid (2 mL) was added dropwise into an acetone solution (80 mL) of 4ACA (3.26 g, 19.99 mmol) in acetone (80 mL) to produce 4-aminocinnamic acid hydrochloride (4ACA hydrochloride). Mixture solution of 4ACA hydrochloride and

hexane (50 mL) were placed in 100 mL round bottom flask and irradiated (250-450 nm, 2.7 mW/cm^3, Marcury lamp) for 30-40 hours to induce [2+2] photocycloaddition. As a result, 4,4'-diamino-α-truxillic acid dihydrochloride was form. M.p.: 178.0 °C. ^{1}H NMR (400 MHz, DMSO-d_6, δ ppm): 3.82 (dd, 2H, *J* =7.7, 9.6), 4.30 (dd, 2H, *J* = 7.7, 9.6 Hz), 7.33 (d, 4H, *J* = 7.7 Hz), 7.45 (d, 4H, *J* = 7.7 Hz), 10.37 (s, 6H), 12.07 (s, 2H). ^{13}C NMR (400 MHz, DMSO-d_6, δ ppm): 40.4, 46.0, 122.8, 128.9, 130.6, 139.1, 172.6.

Recrystallization of 4,4'-diamino-α-truxillic acid dihydrochloride A single crystal was obtained from dispersion liquid of crude 4,4'-diamino-α-truxillic acid dihydrochloride in conc. HCl aqueous, refluxed for 10 min and then cooled to room temperature. Pure sample was obtained as needle crystal. Crystal data: 0.50 x 0.10 x 0.06 mm, $C_{18}H_{20}Cl_2N_2O_4$, colourless, *fw* = 399.26, triclinic, P2(1)/n, *a* = 5.6577(11) A°, *b* = 7.6483(16) A°, *c* = 12.102(3) A°, α = 105.024(12)°, β = 94.685(12)°, γ = 105.769(8) °, *V* = 480.16(19) A°^{3}, *Z* = 1, 1.381 mg/m^3, T = 296(2) K, R_1(I>2σ(I)) = 0.0442, ωR2 (all data) = 0.1250, GOF = 1.019. Single crystal X-ray crystallographic diffraction data were collected a Bruker Smart APEX II CCD area-detector diffractometer, with Mo Kα radiation source (λ = 0.71073 A°) at 296 K. The crystal structures were solved by the directed method with SHELXS-97 program. The full matrix least squares procedures using SHELXL-97 on F^2 anisotropic for all non-hydrogen atom was used to refine the crystal structures [35]. Hydrogen atoms were placed in their calculated positions and refined following the riding model.

Supplementary Material Crystallographic data for the 4,4'-diamino-α-truxillic acid dihydrochloride (CCDC 934691) reported in this article have been deposited with Cambridge Crystallographic Data Centre. These data can be obtained free of charge www.ccdc.cam.ac.uk/data_request/cif, by e-mailing data_request@ccdc.cam.ac.uk, or

by contacting Cambridge Crystallographic Data Centre, 12 Union Road, Cambridge CB2 1EZ, UK, 716905; Fax: +44 1223 336033.

2.2.3.2 Synthesis of 4,4'-diamino-α-truxillic acid methylester 4,4'-diamino-α-truxillic acid methylester was synthesized as follows. 4,4'-diamino-α- truxillic acid dihydrochloride (3.00 g, 7.54 mmol) was mixed with trimethylsilyl chloride ($(CH_3)_3SiCl$) (1.63 g, 5.08 mmol) and methanol (12.20 ml, 0.32 mol) in a two-necked round-bottomed flask under a nitrogen atmosphere at room temperature. The reaction proceeded in a dispersion state at first, but as a result of esterification the products got dissolved in methanol. The reaction mixture was precipitated and dissolved into water and extracted by ethylacetate. The collecting ethylacetate organic layer was dried over $MgSO_4$, and then was evaporated and neutralized using 1 N NaOH. M.p.: 193 °C. ^{1}H NMR (400 MHz, DMSO-d_6, δ ppm): 3.27 (s, 6H), 3.72 (dd, 2H, J = 7.4, 10.2 Hz), 4.11 (dd, 2H, J = 7.4 Hz, 10.1 Hz), 5.00 (s, 4H), 6.51 (d, 4H, J = 8.4 Hz), 6.95 (d, 4H, J = 8.4 Hz). ^{13}C NMR (100 MHz, DMSO-d_6): δ 40.4, 46.6, 51.0, 113.7, 125.7, 128.0, 147.3, 172.1. FT-ICR MS (ESI) calcd for [M+H, $C_{20}H_{23}N_2O_4$]$^+$: 355.1658, found 355.1663.

2.2.3.3 Synthesis of 4,4'-diamino-α-truxillic acid ethylester The 4,4'-diamino-α-truxillic acid ethylester was prepared by an analogous procedure to 2.2.3.2. However, instead of methanol, ethanol was used as a reactant and solvent under a nitrogen atmosphere at reflux temperature. M.p.: 137 °C. ^{1}H NMR (400 MHz, DMSO-d_6, δ ppm): ^{1}H NMR (400 MHz, DMSO-d_6, δ ppm): 0.84 (t, 6H, J= 7.0 Hz), 3.68 (dd, 2H, J= 7.2, 7.2 Hz), 3.73 (q, 4H, J= 6.8 , 7.6 Hz), 4.10 (dd, 2H, J = 7.2, 7.6 Hz), 4.96 (S, 4H), 6.49 (d, 4H, J = 8.4 Hz), 6.95 (d, 4H, J = 8.4 Hz). ^{13}C NMR (400 MHz, DMSO-d_6, δ ppm): 13.7, 40.3, 46.5, 59.6, 113.5, 125.7, 128.1, 147.3, 171.6. FT-ICR MS (ESI) calcd for [M+H, $C_{22}H_{27}N_2O_4$]$^+$: 383.468, found 383.1300.

2.2.4 Polyamide synthesis

Typical example of syntheses of aromatic polyamide was given for the synthesis of polyamide from 4,4'-diamino-α-truxillic acid dimethylester with dipicolic acid. 4,4'-diamino-α-truxillic acid dimethylester (0.20 g, 0.56 mmol) placed in a round bottom flask under nitrogen atmosphere, anhydrous NMP (0.56 mL), anhydrous pyridine (560 μL), $(PhO)_3P$ (160 μL) and dipicolic acid (0.09 g, 0.56 mmol) were added. After the reaction mixture was stirred for 24 hours at 110 °C, the solution was diluted in NMP (3 mL), and then dropped into ethanol (100 mL) to precipitate. The obtained fibril was dried in reduced pressure and determined to be polyamides.

2.2.5 Molecular weight of polyamide

The number average molecular weight (M_n), the weight average molecular weight (M_w) and the molecular weight distribution of polyamide (PDI) were determined by gel permeation chromatography (GPC, conc. 5 mg/L, DMF as an eluent) after calibrated with the standard pullulans at 40 °C.

2.2.6 TGA and DSC measurement

The thermal properties of the polyamide were analyzed by TGA (Seiko Instruments Inc., SSC/5200 SII) and DSC (Seiko Instruments Inc., EXSTAR X-DSC7000 SII). Polyamide was dried at 100 °C for 1 h to remove the absorbed moisture before measuring TGA and DSC. The thermal degradation behavior of polyamide (T_5 and T_{10}) was investigated by heating from 50 °C to 750 °C at a rate of 10 °C/min under a nitrogen atmosphere. For the DSC measurement, both the heating and cooling rates were 10 °C/min under a nitrogen atmosphere and the temperature

ranged from 50 °C to 300 °C. One sample measurement was carried three cycles of heating and cooling rate. The T_g (glass transition temperature) was obtained from DSC curves of second heating cycle.

2.3 Results and Discussion

2.3.1 Monomer Syntheses

Interestingly, 4,4'-diamino-α-truxillic acid dihydrochloride was synthesized by a perfect [2+2] photocycloaddition of 4ACA hydrochloride salt (scheme 2.1). The cyclobutane ring of α-truxillic acid, a dimer, was occurred with ultraviolet light source above 260 nm which was stable at elevated temperature [36]. However, photolabile under deep ultraviolet light, below 260 nm, cyclobutane was cleaved to the intitial of 4ACA. The crude of 4,4'-diamino-α-truxillic acid dihydrochloride was recrystallized by treating with conc. HCl at refluxed temperature to receive the small needles with white color (Figure 2.1c).

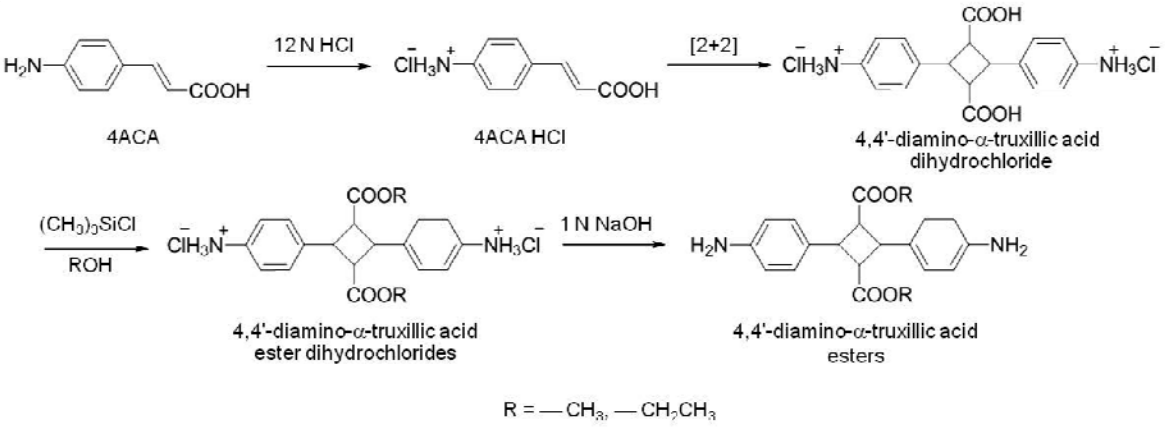

Scheme 2.1 Syntheses of the 4,4'-diamino-α-truxillic acid methylester and ethylester.

Figure 2.1 The physical appearance of (a) 4ACA (b) the crude of 4,4'-diamino-α-truxillic acid dihydrochloride and (c) the crystal of 4,4'-diamino-α-truxillic acid dihydrochloride.

4ACA showed dark yellow powder while the crude of 4,4'-diamino-α-truxillic acid dihydrochloride showed only pale yellow powder (Figure 2.1a and b).

The photodimerized structure was confirmed by ^{1}H NMR, ^{13}C NMR and X-ray crystallography. A single crystal X-ray diffraction study of 4,4'-diamino-α-truxillic acid dihydrochloride (Figure 2.2), which was formed in conc. HCl, confirmed the molecular structure. The molecular structure was *trans*-configuration. One cyclohexane located opposite site of a plane of another cyclohexane ring. Atomic position parameters were presented in Table A1, and bond lengths and angles were given in Table A2.

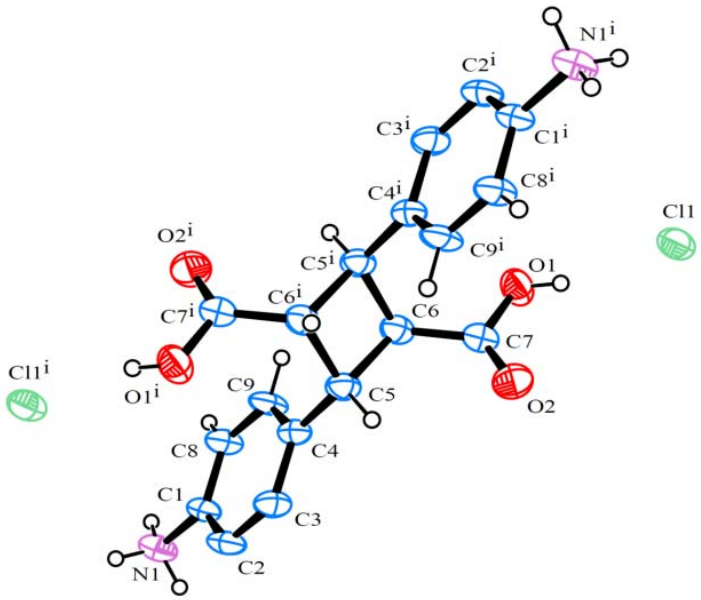

Figure 2.2 The molecular structure of 4,4'-diamino-α-truxillic acid dihydrochloride by using X-ray crystal spectrometer.

Figure 2.3 showed ^{1}H NMR spectra of 4ACA (Figure 2.3a) and products via [2+2] photocycloaddition. 4,4'-diamino-α-truxillic acid dihydrochloride (Figure 2.3b) showed that photo-irradiation resulted in disappearance of vinylene proton signals around 7.44-7.40 and 6.15-6.12 ppm and instead appearance of cyclobutane proton signal around 4.33-3.81 ppm, while proton signals assigned to carboxylic acids, amines, and aromatics shifted slightly. When 4ACA in a non-salt state was photo-irradiated, no reaction occurred. The salt state of 4ACA was very important to react quantitatively. 4,4'-diamino-α-truxillic acid dihydrochloride has two amine groups but two carboxylic acids and then was difficultly used as a monomer for polyamide and polyimides (PIs). Then 4,4'-diamino-α-truxillic acid dihydrochloride was subsequently esterified in the dispersion state of reactant alcohol solvents such as methanol and ethanol in the presence of $(CH_3)_3SiCl$. If 4ACA was esterified, the products were dissolved in the solvents to react smoothly. As a result, ^{1}H NMR signals of these alkyl esters were confirmed as shown in Figure 2.3c (4,4'-diamino-dimethyl-α-truxillic acid methylester) and Figure

2.3d (4,4'-diamino-diethyl-α-truxillic acid ethylester). Moreover, the expected structures of both 4,4'-diamino-α-truxillic acid ester hydrochlorides were also confirmed by ^{13}C NMR (Figure 2.4), ^{1}H-^{13}C NMR HSQC and HMBC spectra (Figure 2.5).

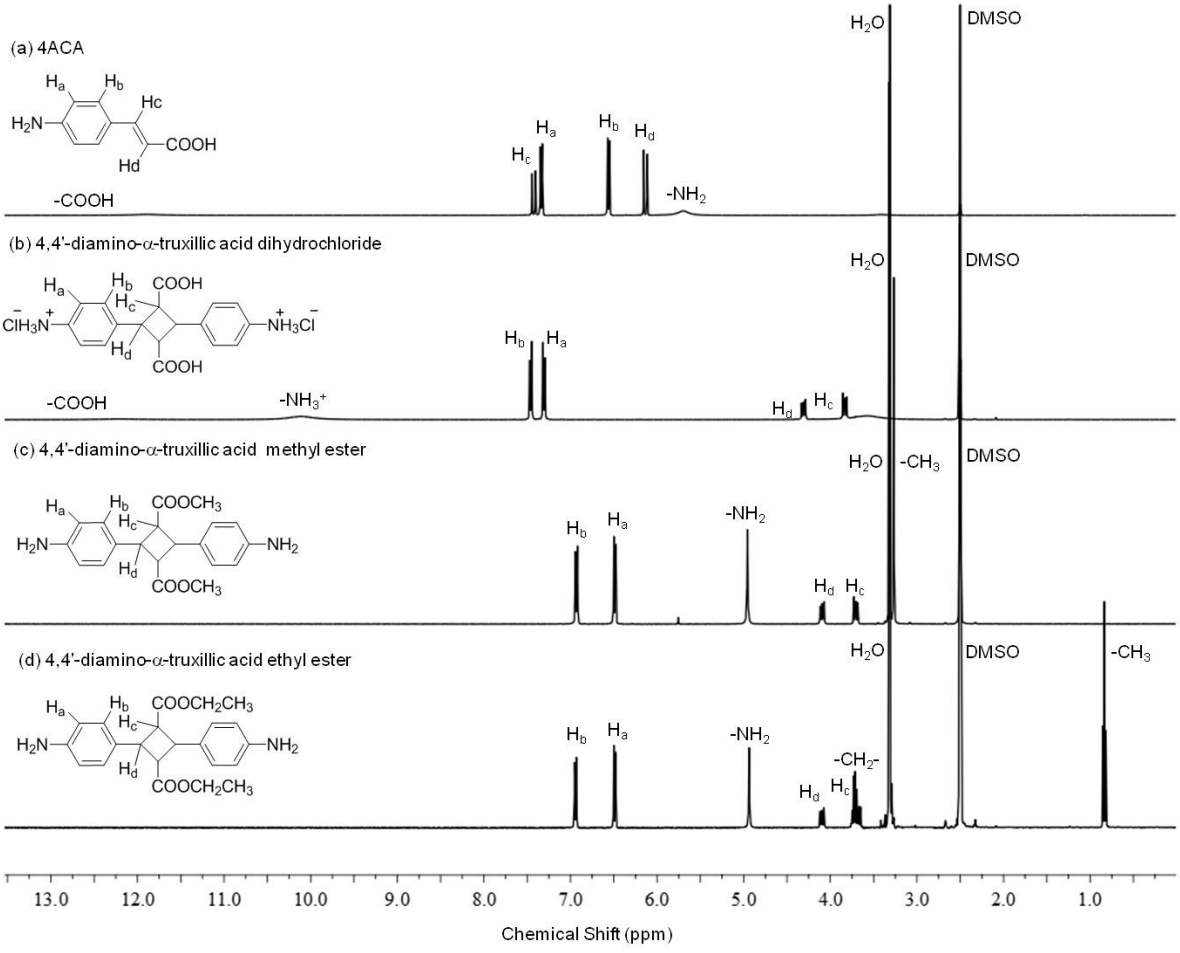

Figure 2.3 ^{1}H NMR spectra of (a) 4ACA (b) 4,4'-diamino-α-truxillic acid dihydrochloride (c) 4,4'-diamino-α-truxillic acid methylester and (d) 4,4'-diamino-α-truxillic acid ethylester.

As to the ^{13}C NMR, the resonance signals of 4,4'-diamino-α-truxillic acid dihydrochloride showed seven main signals (Figure 2.4a), while those of 4,4'-diamino-α-truxillic acid methylester dihydrochloride (Figure 2.4b) and 4,4'-diamino-α- truxillic acid ethylester dihydrochloride (Figure 2.4c) showed more than seven signals that belonged to methyl group at 46.6 ppm and ethyl group at 59.6 and 13.7 ppm, respectively.

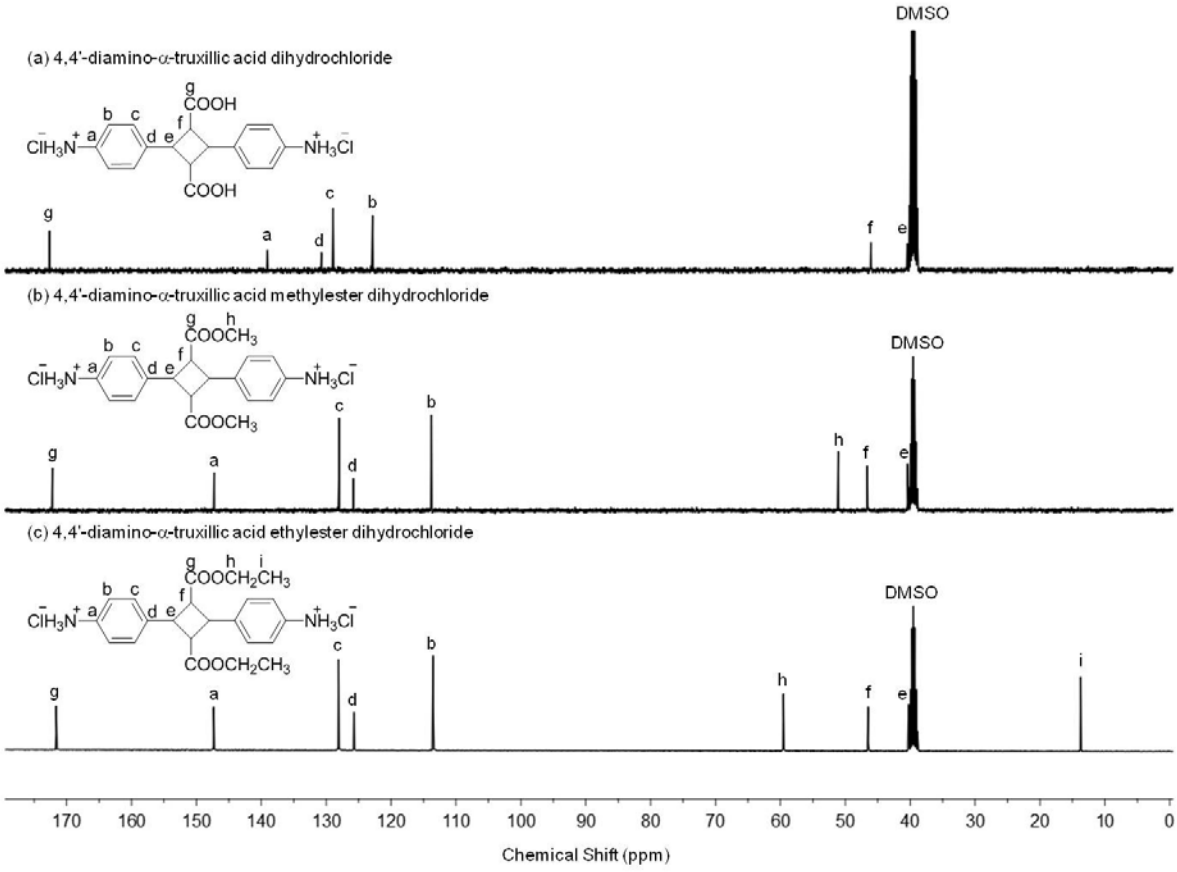

Figure 2.4 ^{13}C NMR spectra of (a) 4,4'-diamino-α-truxillic acid dihydrochloride (b) 4,4'-diamino-α-truxillic acid methylester dihydrochloride and (c) 4,4'-diamino-α-truxillic acid ethylester dihydrochloride.

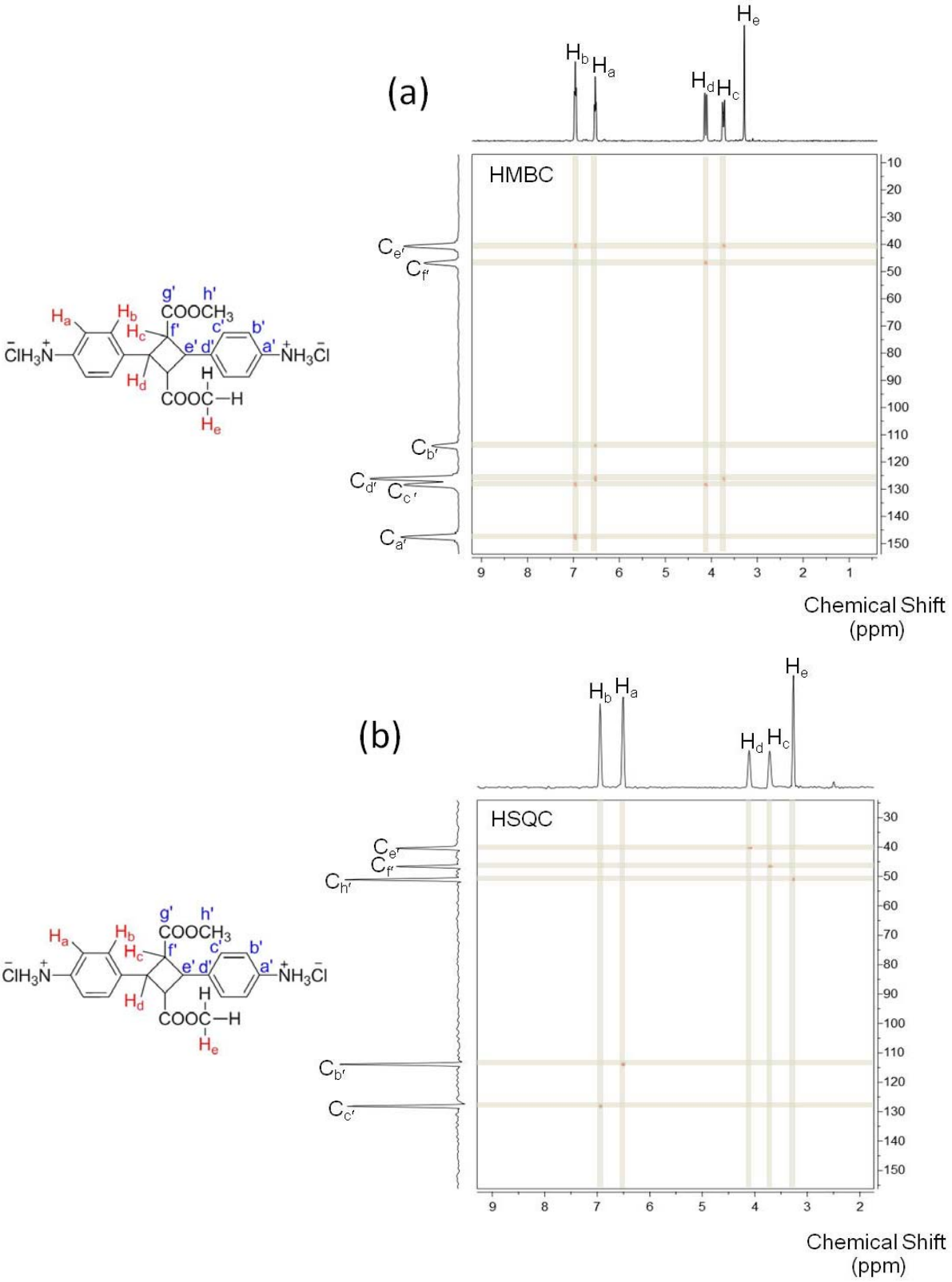

Figure 2.5 (a) ^{1}H-^{13}C NMR HMBC and (b) ^{1}H-^{13}C NMR HSQC spectra of 4,4'-diamino-α-truxillic acid methylester hydrochloride.

As to ^{1}H-^{13}C NMR HSQC and HMBC spectra of 4,4'-diamino-α-truxillic acid methylester hydrochloride focused on the correlation between aromatic, cyclobutane and methyl of protons and carbon thirteen. This technique was used to confirm proton of cyclobutane position on ^{1}H NMR spectrum which was related to chemical shift at 3.82 ppm (H_c) and 4.30 ppm (H_d).

FTIR spectra of 4,4'-diamino-α-truxillic acid dihydrochloride, 4,4'-diamino-α-truxillic acid methylester and ethylester were showed in Figure 2.6. A broad hydroxyl peak at 2865 cm^{-1} was disappeared and carbonyls at 1700 cm^{-1} (Figure 2.6a) shifted toward the higher wavenumber at 1713 cm^{-1} (Figure 2.6b and c) as a result of carboxylic acid reaction to be esters.

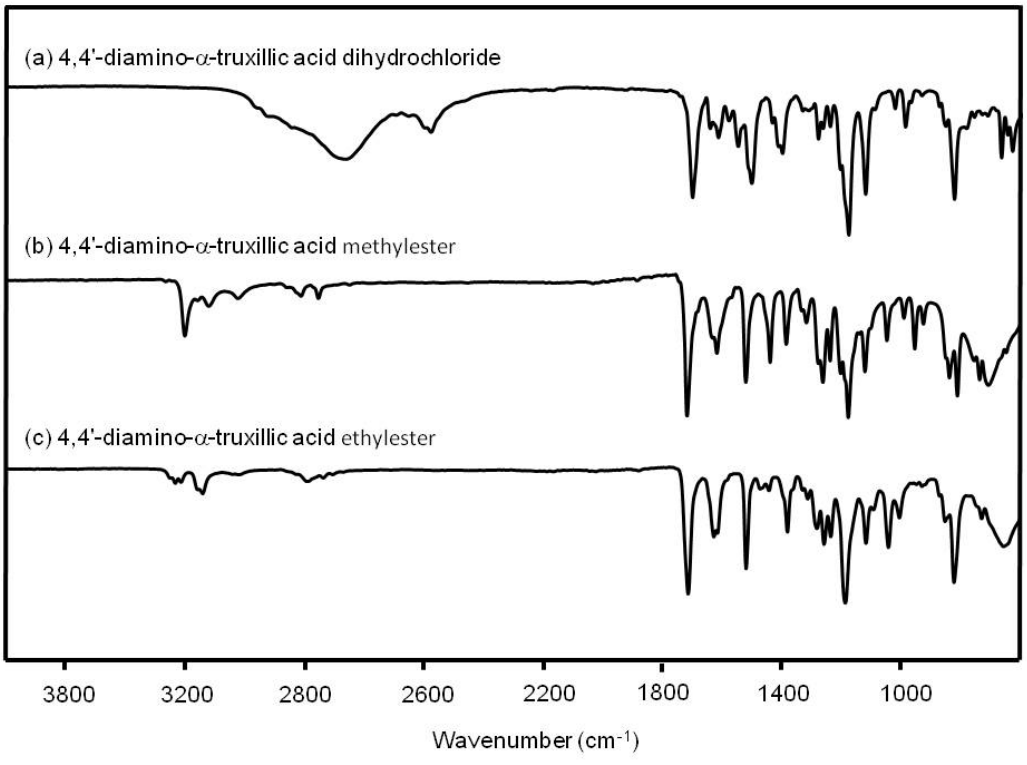

Figure 2.6 FTIR spectrum of (a) 4,4'-diamino-α-truxillic acid hydrochloride (b) 4,4'-diamino-α-truxillic acid methylester and (c) 4,4'-diamino-α-truxillic acid ethylester.

2.3.2 Synthesis and characterization of polyamide

The reaction route of polyamide synthesis (scheme 2.2) was interested because polyamide was synthesized from both bioavalible compounds. Polyamide was prepared based on a polycondensation using $(PhO)_3P$ and pyridine as coupling agent in NMP at 110 °C under nitrogen atmosphere for 24 hours. The result product showed a yellow solution which was not showed obvious change in viscosity.

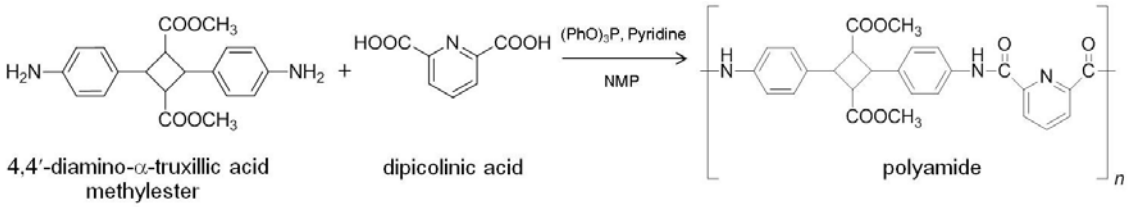

Scheme 2.2 Synthesis of the fully bio-based polyamide from 4,4'-diamino-α-truxillic acid methylester and dipicolic acid.

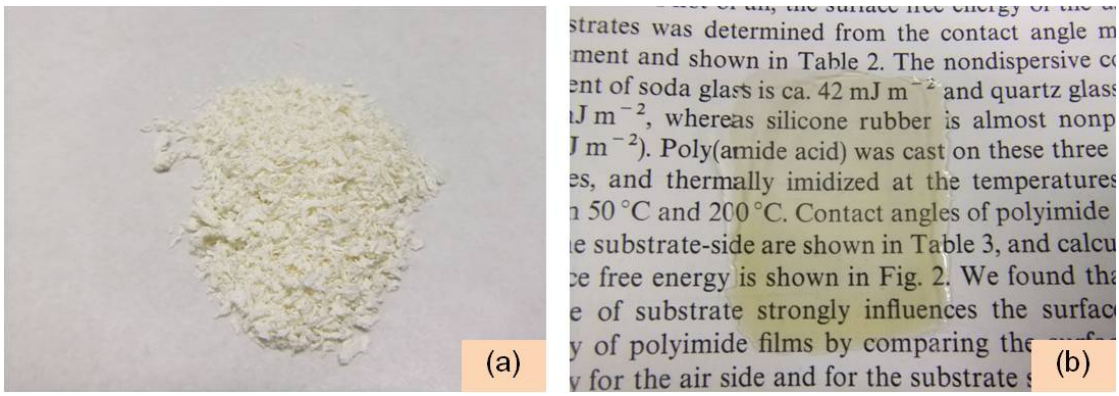

Figure 2.7 physical appearances of polyamide (a) fibrils and (b) film**.**

Polyamide fibrils were prepared by precipitation of polyamide solution in ethanol and dried under vacuum overnight. They appeared white fibrils (Figure 2.7a) and then dissolved polymer fibrils with concentration of 0.2 g/mL in NMP. Polymer solution was casted on glass plate and heat at 60-70 °C. The obtained polyamide

showed yellow color transparency and flexible film (Figure 2.7b).

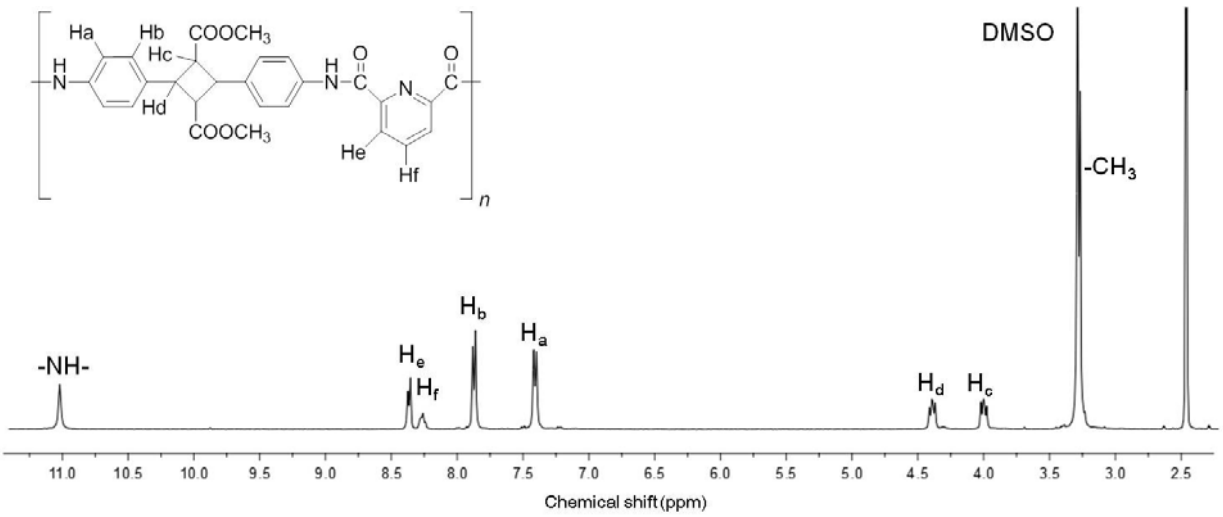

Figure 2.8 ^{1}H NMR spectrum of polyamide.

^{1}H NMR and FTIR were used to characterize polyamide structure. The ^{1}H-NMR signals (Figure 2.8) showed the presence of amine proton at 11.1 ppm, the aromatic dicarboxylic protons and the aromatic diamine protons of benzene ring were observed in the range of 8.3-8.4 ppm and 7.4-7.9 ppm, respectively. Cyclobutane protons were assigned at 4.0-4.5 ppm and methyl proton was slightly overlapped with water at 3.3 ppm.

The FTIR spectra of polyamide (Figure 2.9) showed the amide region at 3361 cm^{-1} (N-H stretching of amide), the alkyl absorption peak of the diamines at 2957 cm^{-1} (C-H stretching of methylester), the benzene ring absorption of diamines and dipicolinic acid at 1525 cm^{-1} (C=C stretching of aromatic ring) and 1436 cm^{-1} (C-H overtone aromatic ring). Moreover, it showed the characteristic absorption of polyamide at 1729 cm^{-1} (C=O symmetric stretching of amide), 1685 cm^{-1} (N-H bending of amide) and 3° amine absorption peak of dipicolinic acid at 1327 cm^{-1} (C-N stretching of aromatic amine). These result indicated the expected polyamide.

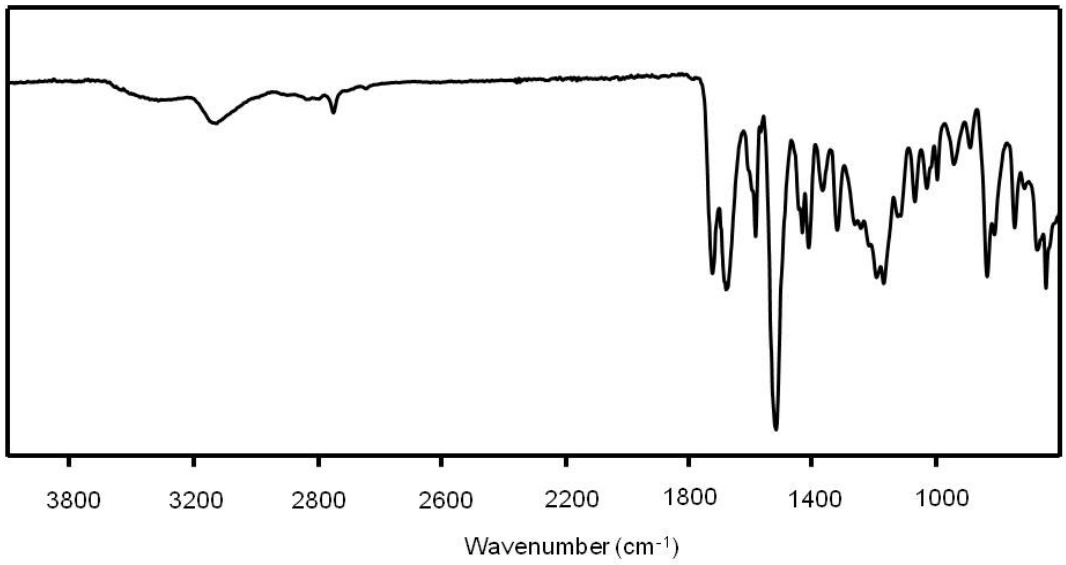

Figure 2.9 FTIR spectrum of polyamide.

2.3.3 Molecular weight of Polyamide

The molecular weights of polyamide were estimated in DMF by GPC. The number average molecular weight, weight average molecular weight and PDI were M_n = 2.03 × 10^4, M_w = 2.98 × 10^4 and PDI = 1.47, respectively. The obtained polyamide showed low molecular weight.

2.3.4 Thermal properties of Polyamide

The thermal properties of the polyamide were analyzed by TGA (Figure 2.10) and DSC (Figure 2.11). For industrial applications, the thermal properties of polyamide were important. Figure 2.10 showed a thermogravimetry curve, the 10 % weight loss temperature was observed at 373 °C. In addition, from differential scanning calorimetry (DSC) analysis, the glass transition temperature of the polymer was detected at 282 °C. These thermostability values are high enough to apply this polyamide as a super-engineering plastic.

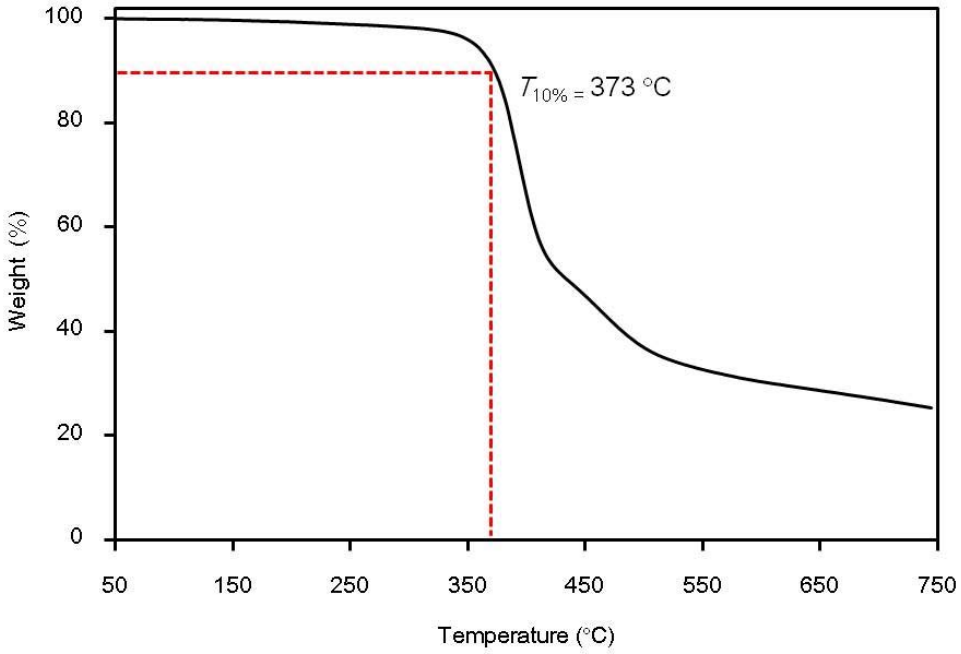

Figure 2.10 TGA curves of polyamide (under a nitrogen atmosphere, 10 °C/min).

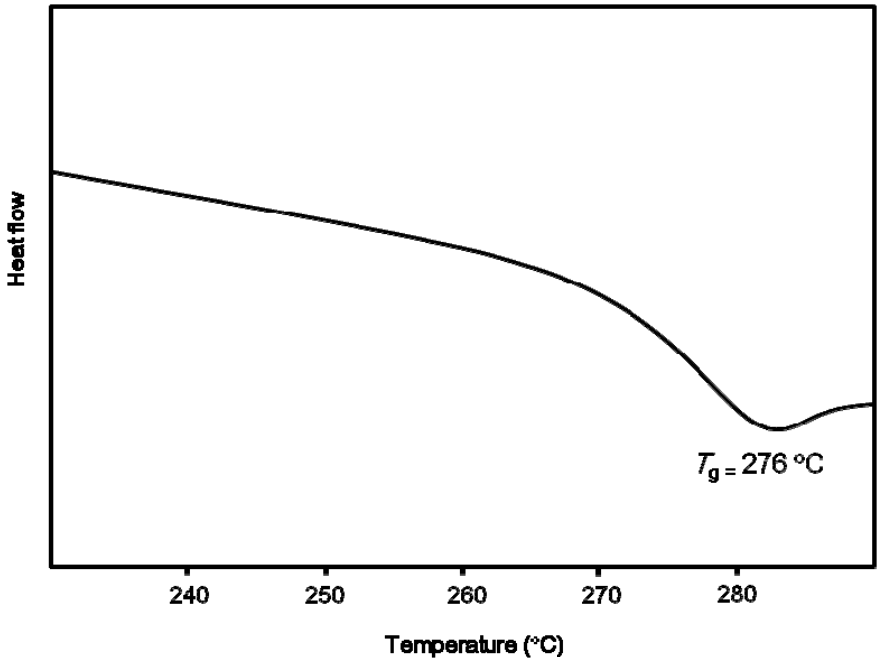

Figure 2.11 DSC curves of polyamide (under a nitrogen atmosphere, 10 °C/min)

2.3.5 Mechanical properties of Polyamide

Mechanical properties of polyamide were measured by a tensile test. The polyamide films had tensile strength in the range of 62 MPa, tensile modulus in the range of 2.8 GPa, and elongation at break in the range of 1.9%.

2.3.6 Solubility test of Polyamide

As listed in the table 2.1, polyamide was soluble in polar aprotic solvent, for example, NMP, DMAc, DMF and DMSO and polar protic solvent, such as, conc. sulfuric acid at room temperature. Nevertheless, polyamide was partial soluble in polar aprotic solvent such as THF and non-polar solvent such as chloroform and dichloromethane at 60 °C. These results could be confirmed that PIs have high chemical resistance.

Table 2.1 Solubility behavior of Polyamide

Solvents								
H_2O	MeOH	EtOH	$(CH_3)_2CO$	CH_3CN	DMF	NMP	DMAc	DMSO
−	−	−	−	−	+	+	+	+

Solvents							
Toluene	Hexane	THF	$CHCl_3$	$(C_2H_5)_2O$	CH_2Cl_2	EtOAc	Conc.H_2SO_4
−	−	±	±	−	±	−	+

+:Soluble at room temperature, ±: Partially soluble at 60 °C, −: Insoluble at 60 °C

$(CH_3)_2CO$ is acetone, CH_3CN is acetonitrile, $CHCl_3$ is chloroform, $(C_2H_5)_2O$ is diethyl ether, THF is tetrahydrofuran, CH_2Cl_2 is dichloromethane, EtOAc is ethylacetate

2.4 Conclusion

New kind of bio-derived diamines from 4ACA, i.e. 4,4'-diamino-α-truxillic acid methylester and ethylester, were successfully prepared from photocycloaddition. ^{1}H NMR, ^{13}C NMR, ^{1}H-^{13}C NMR HMBC, ^{1}H-^{13}C NMR HSQC, FTIR and FT-ICR MS were used to characterize diamine structure. A single crystal X-ray diffraction also used to confirm the *trans*-molecular configuration of diamine under UV irradiation. The resulting diamines were employed to react with bioavaliable dipicolic acid in presence of NMP to form a polyamide which was characterized by ^{1}H NMR and FTIR. Polyamide showed high T_{10} and T_g at 373 °C and 276 °C, respectively. Although polyamides showed high thermal stability, they were easy to hydrolysis which was not suitable to use as manufacture. Next chapter, I explained about syntheses bio-based polyimides to overcome these problem and used as high performance material and various applications.

CHAPTER 3

SYNTHESES AND CHARACTERIZATION OF BIO-BASED POLYIMIDES DERIVED FROM 4-AMINOCINNAMATE BIOCHEMICALS WITH THEIR THERMO-MECHANICAL PROPERTIES

CHAPTER 3
SYNTHESES AND CHARACTERIZATION BIO-BASED POLYIMIDES DERIVED FROM 4-AMINOCINNAMATE BIOCHEMICALS WITH THEIR THERMO-MECHANICAL PROPERTIES

3.1 Introduction

Recently, demand for high performance polymers has increased due to their excellent thermal and chemical stability, radiation resistance, good mechanical properties and low dielectric constant [37]. Polyimide (PI) is one of the most vital classes of high performance polymers which can be used as super-engineering plastics in a variety modern industrial and commercial applications such as in electronic industry, adhesive, laminating resin, film or coating and aerospace [1]. Another property of PI is low coefficient of thermal expansion in organic compound and few errors from expansion with used at high temperature which was suitable for use in wider processibility window [38]. Factors that contribute PI to high performance polymers are presented such as resonance stabilization, molecular symmetry, high molecular weight and high molecular distribution, rigid intrachain structure, mechanism of bond cleavage and additives or reinforcements (fillers, clays, miscellaneous nanoparticles) [39]. However, most PI is produced from petrochemicals which currently have serious problems associated with the limited amount of them. In addition, they have long term resistance to degradation by living system resulting in environmental problems. Therefore, development of bio-derived environmentally benign PIs are extremely interesting because it can reduce the amounts petroleum consumption and plastic dust

by decomposition by environmental functions such as sun, light, rain and biological activity such as microorganism.

4-aminocinnamic acid (4ACA) is biological compound derived from glucose by using enzyme bioactivity such as microorganism. [2+2] photodimerization of 4ACA can be converted to starting materials in order to synthesize bio-based monomers. The benefit of using the light as a remote stimulus is an attractive nano-object disassembling driving force, which has been intensively investigated for accurately targeted and highly selective [36].

Here, we tried to describe the new concept of synthesized the aromatic diamine monomers from bio-derived 4ACA. Even though the aromatic diamines are difficult to derive from bioorganisms due to their toxicity, this research can be first used. Photochemical dimerization of 4ACA conduce the formation of new dimers by the reaction of two unsaturated 4ACA. New aromatic diamine dimers were used for PIs syntheses as following. PI from aromatic diamines were synthesized with tetracarboxylic dianhydride, such as 1,2,3,4-cyclobutane tetracarboxylic dianhydride (CBDA), pyromellitic dianhydride (PMDA), 3,3',4,4'-benzophenone tetracarboxylic dianhydride (BTDA), 4,4'-oxydiphthalic anhydride (OPDA), 3,4,3',4'-biphenyltetracarboxylic dianhydride (BPDA) and 3,3',4,4'-diphenylsulfone tetracarboxylic dianhydride (DSDA) by using polycondensation procedure. The variation in the structure of aromatic diamines and dianhydrides had a dramatically effect on the properties of PI like T_g and T_m toward understanding these structure-property relationships. The resulting PIs were concerned about high heat resistance and high mechanical property. Moreover, the optical properties, chemical resistance and cell adhesion of PIs were discussed in chapter 4.

3.2 Experimental Section

3.2.1 Materials

4-aminocinamic acid (4ACA) and pyromellitic dianhydride (PMDA) were purchased from TCI (Tokyo, Japan). 1,2,3,4-Cyclobutane tetracarboxylic dianhydride (CBDA), 3,3',4,4'-benzophenone tetracarboxylic dianhydride (BTDA), 4,4'-oxydiphthalic anhydride (OPDA), 3,4,3',4'-biphenyltetracarboxylic dianhydride (BPDA), 3,3',4,4'-diphenylsulfone tetracarboxylic dianhydride (DSDA), trimethylsilyl chloride ($(CH_3)_3SiCl$) and *N*,*N*-dimethylacetamide (DMAc, 99.8 % anhydrous) were purchased from Aldrich Chemical. Hydrochloric acid (HCl), sodium hydroxide (NaOH) and sodium sulfate (Na_2SO_4) were purchased from Kanto Chemical and used as chemical reagent and drying agent. All of dianhydrides were purified by treating with acetic anhydride, heating at reflux temperature for 5 h, cooling to 0-5 °C and collecting the dianhydride, washing by hot dioxane. The moisture sensitive solid were collected and dried in *vacuo*. All other reagents such as methanol, ethanol, acetone and hexane were obtained from various commercial sources and used as a solvent for reactions.

3.2.2 Poly(amic acid) Syntheses

A typical polymerization procedure for the synthesis of poly(amic acid) (PAA) was synthesized by addition polymerization of equimolar amounts of dianhydride and diamine in DMAc as follows. 4,4'-diamino-α-truxillic acid methylester, (0.20 g, 0.5647 mmol) were dissolved in DMAc (0.5647 mL, 0.6 M) in a 10 mL-test tube under a nitrogen atmosphere. Dianhydrides such as CBDA (0.11 g, 0.5647 mmol), PMDA (0.11 g, 0.5235 mmol), BTDA (0.18 g, 0.5650 mmol), OPDA (0.18 g, 0.5648), BPDA (0.17g, 0.5642 mmol), DSDA (0.20 g, 0.5660 mmol) was added into diamine solution. The

reaction mixture was vigorous stirred at room temperature for 48 h to produce a pale yellow solution to yield a viscous PAA solution. The PAA solution was diluted in DMAc, and then added dropwise into ethanol to precipitate PAA fibrials which was collected by filtration, thoroughly washed with water and dried in a vacuum oven for 12 h. PAA film was obtained by casting a DMAc yellow solution onto a silicon wafer and dried by heating at 60-70 °C. The PAA specimen for UV-Vis measurements was prepared by spin-casting method (spin rate: 1000 rpm, MS-A100 Spincoater, Mikasa Co., Ltd.) to adjust the thickness to be ~9-15 μm. The ^{1}H NMR measurements were performed by Bruker Biospin AG 400 MHz, 54 mm spectrometer using DMSO-d_6 as solvent.

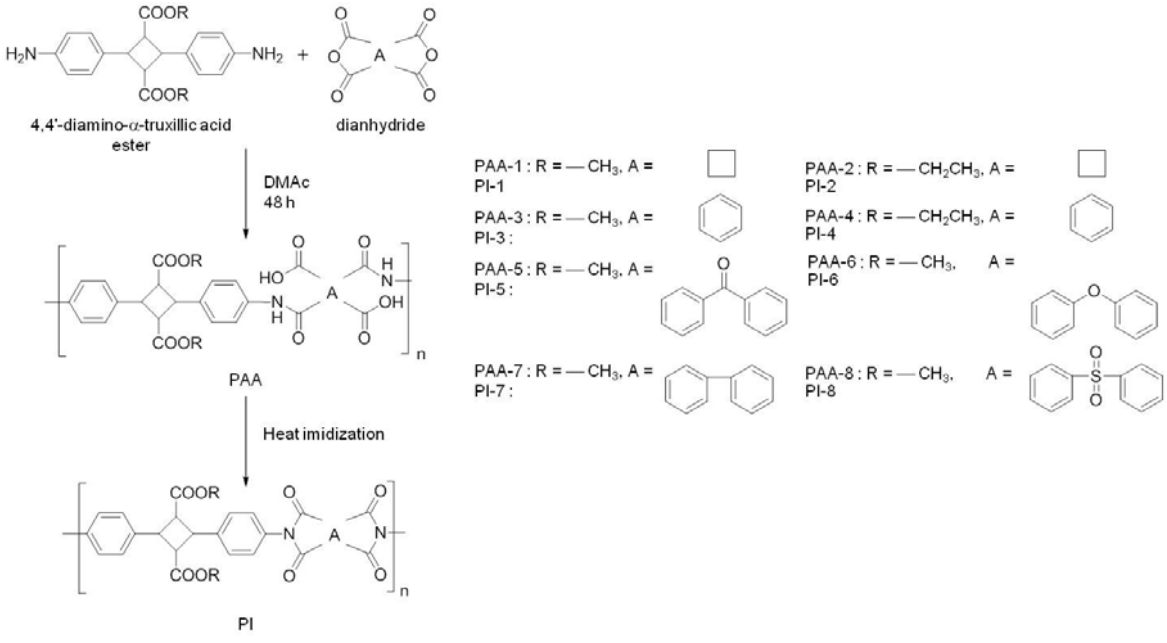

Scheme 3.1 Syntheses of PAAs and PIs.

3.2.3 Polyimide Syntheses

Polyimide (PI) films were obtained by thermally imidization of the PAAs in an oven under vacuum by stepwise heating at 100, 150, 200 and 250 °C for 1 hr at each step.

3.2.4 Polymer Characterization

FT-IR spectra were recorded with Perkin Elmer Spectrum One spectrometer between 4000-600 cm^{-1} using a diamond-attenuated total reflection (ATR) accessory. X-ray diffraction (XRD, RINT 2000 and Rigaku) was used to determine degree of crystallization of PI films by using Gram AI program.

3.2.5 Polymer viscosities and Molecular weight

Inherent viscosities of polymer were measured using Ubbelohde viscometer at 30 °C in DMAc at a polymer concentration of 0.5 dL/g. The number average molecular weight (M_n), the weight average molecular weight (M_w) and the molecular weight distribution of polymer (PDI) determined by gel permeation chromatography (GPC, conc. 5 g/L, DMF as an eluent) after calibrated with the standard pullulans at 40 °C.

3.2.6. Density and Mechanical properties

Film preparation A total 0.8 g of each PAAs was dissolved in DMAc to a concentration of 0.1 g/mL. The solutions were cast on 5 cm^2 glass plate, and the solvent was allowed to evaporate at 60 °C. All of obtained PAA films were further stepwise increased temperature at 100 °C, 150 °C, 200 °C and 250 °C each 1 h under vacuum becoming PIs.

Density PI films were cut, weighed and measured their size to calculate density by mass per volume ($g.cm^{-3}$).

Tensile testing Tensile specimens were cut from cast films with dimensions of as follows in the Figure 3.1. The tensile measurements such as tensile strength, breaking elongation and tensile modulus were carried out on a tensometer, instron 3365-L5, Canon at room temperature. The maximum load was 5 kN, and the elongation speed was 0.5 $mm.min^{-1}$.

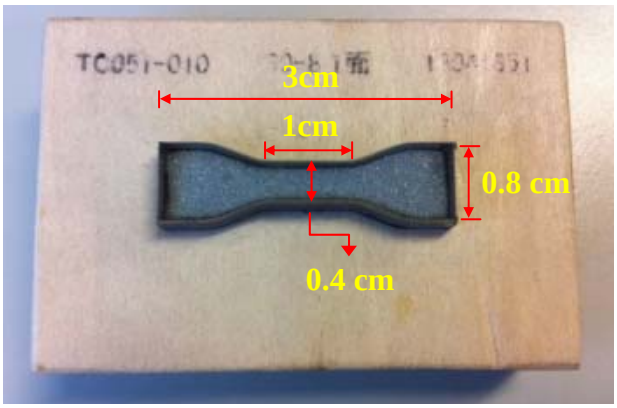

Figure 3.1 Size of film specimen for tensile testing.

3.2.7 TGA and DSC measurement

The thermal properties of the various PIs were analyzed by TGA (Seiko Instruments Inc., SSC/5200 SII) and DSC (Seiko Instruments Inc., EXSTAR X-DSC7000 SII). All of PIs subsequently dried at 100 °C for 1 h to remove the absorbed moisture before measuring TGA and DSC. The thermal degradation behavior of PIs (T_5 and T_{10}) was investigated by heating from 50 °C to 600 °C at a rate of 10 °C/min under a nitrogen atmosphere. For the DSC measurement, both the heating and cooling rates were 10 °C/min under a nitrogen atmosphere and the temperature ranged from 50 °C to

350 °C. One sample measurement was carried three cycles of heating and cooling rate. The T_g (glass transition temperature) was obtained from DSC curves of second heating cycle.

3.2.8 Refractive indices

The refractive indices of thin PI films were evaluated by Abbe refractometer (Atago, NRA, 1T) employing α-bromonapthalene as a contact liquid at room temperature.

3.3 Result and Discussion

3.3.1 Structural Analysis

The PAAs, which were the precursors of PIs, were prepared by the polycondensation of the prepared diamines with stoichiometric amounts of dianhydrides CBDA, PMDA, BTDA, OPDA, BPDA and DSDA (scheme 3.1). After precipitation by ethanol, all of PAAs showed white fibrils as same physical appearance as PAA-1 (Figure 3.2a). Among these dianhydrides, we confirmed that CBDA was converted by Hg-lamp irradiation (λ= 250-450 nm) to maleic acid dimethyl which was bioavailable derivatives, and successively cyclization. PIs were occurred by stepwise heat imidization via PAAs precursors at maximum temperature 250 °C. PIs were dissolved in DMAc and casted on glass plate to prepare PI films. The characteristic of synthesized PIs were showed in Figure 3.2b compared with Kapton™ as commercial polymer. The films become light to thick yellow. It was explicit that PI-1 and PI-2 derived from fully bio-based cyclobutane while others were partially bio-based showed no color and high transparency than Kapton™.

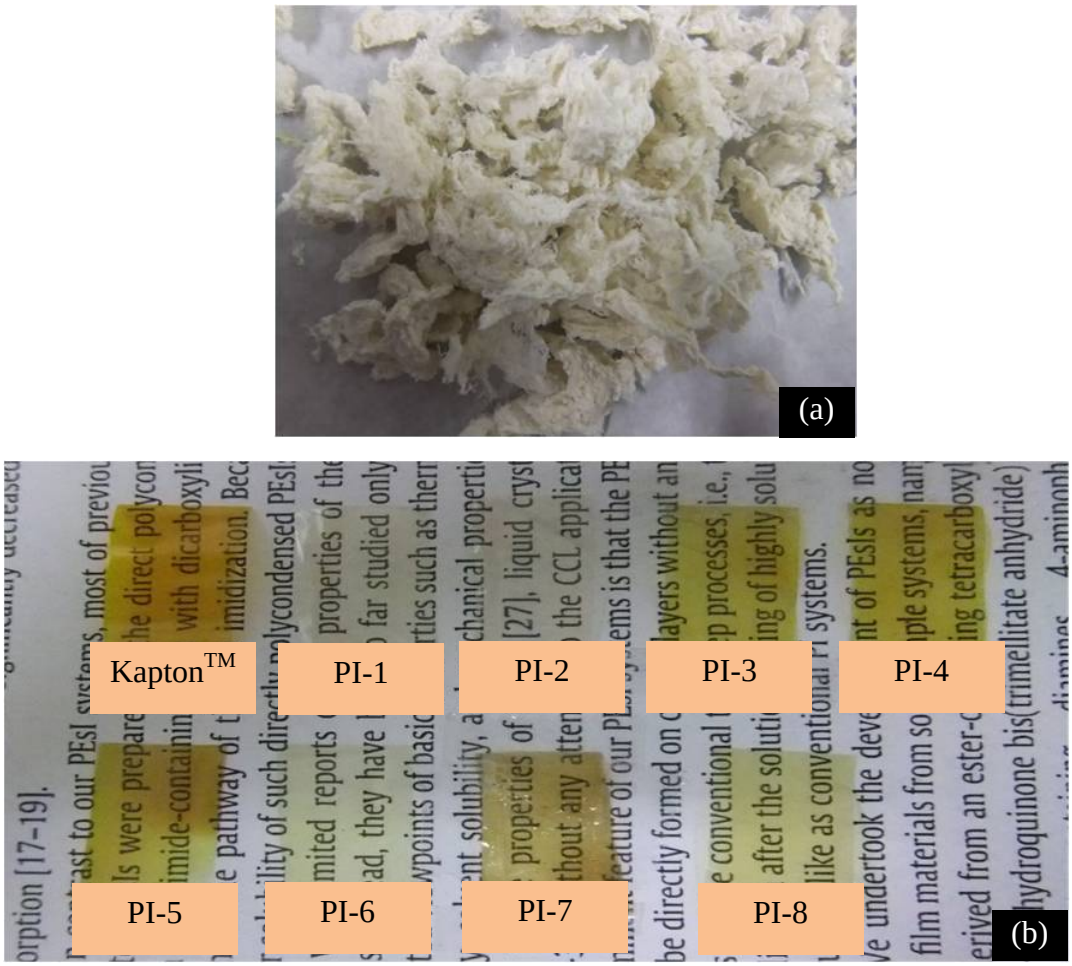

Figure 3.2 Physical appearances of (a) PI-1 fibrils and (b) Kapton™ flim compared with all of PI films.

The ^{1}H NMR spectra of PAAs (Figure 3.3) were assigned the amide protons in the range of 10.6-10.1 ppm, the aromatic diamine protons of benzene ring were observed in the range of 7.6-7.3 ppm, cyclobutane protons at 4.3-3.3 ppm and aromatic dianhydride protons in the range of 8.5-7.3 ppm. Methyl protons of PAAs were overlapped with water at about 3.3 ppm. Nevertheless, PAA-2 and PAA-4 were observed methylene protons at 3.8 ppm and methyl protons at 0.9 ppm. Other PAAs

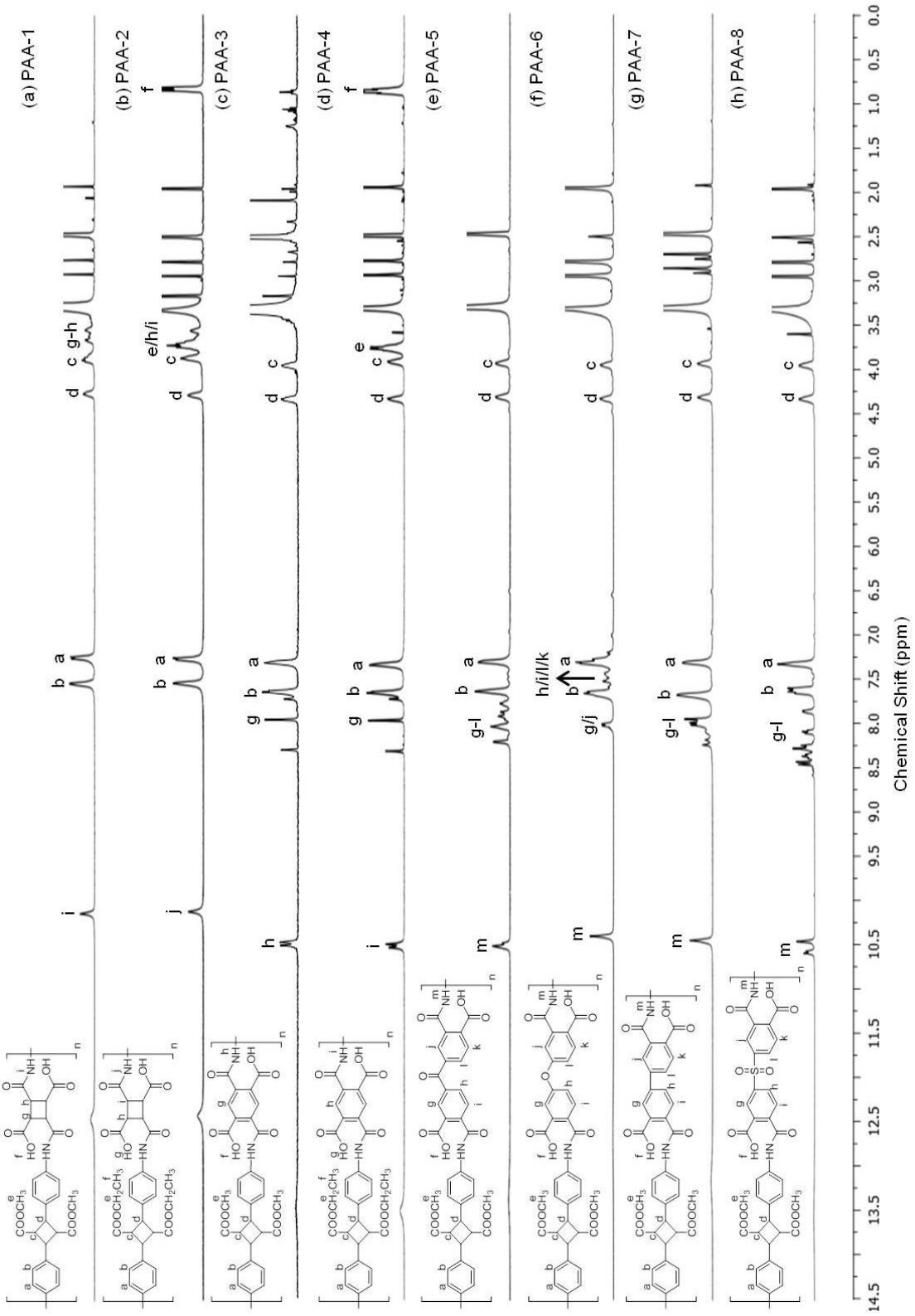

Figure 3.3 ^{1}H NMR spectra of (a) PAA-1 (b) PAA-2 (c) PAA-3, (d) PAA-4 (e) PAA-5 (f) PAA-6 (g) PAA-7 and (h) PAA-8.

showed signals of dianhydride-derived aromatic protons around 8.5-7.3 ppm additionally to abovementioned signal.

The FTIR spectra of PAAs (Figure 3.4) showed broad absorption bands region of 2500 to 3500 cm^{-1} (O-H stretching), the carboxylic absorption peak of the ring-opening dianhydride at 1719 cm^{-1} (C=O stretching, carboxylic), 1668 (C=O stretching, amide) and 1520 cm^{-1}, 1436 cm^{-1} (C-H overtone aromatic), in any samples.

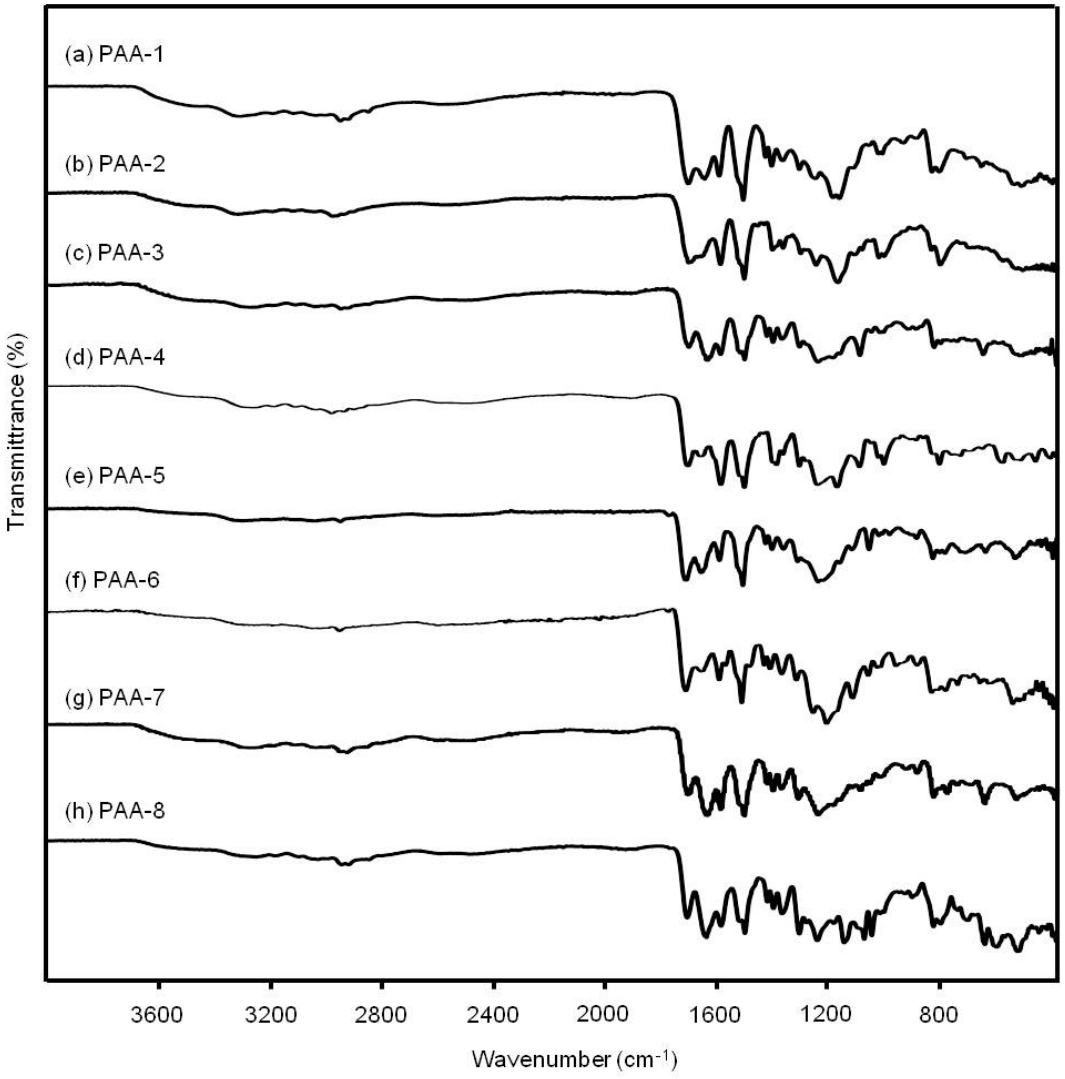

Figure 3.4 FTIR spectra of (a) PAA-1 (b) PAA-2 (c) PAA-3, (d) PAA-4 (e) PAA-5 (f) PAA-6 (g) PAA-7 and (h) PAA-8.

On the other hand, all the annealed PI films were obtained by thermally curing the PAAs (Figure 3.5). They showed double carbonyl absorptions; small peak at 1785 cm^{-1} (C=O asymmetric stretching) and 1716 cm^{-1} (C=O symmetric stretching). Besides, other peaks at 1518 cm^{-1} (C-C stretching of aromatic), 1441 cm^{-1} (C=C stretching of *p*-substituted benzene), 1376 cm^{-1} (C-N stretching of imide), and 1175 cm^{-1} (imide ring deformation) appeared, which indicated the complete imidization [25]. Especially the PIs were abbreviated as PI-1, PI-2, PI-3, PI-4, PI-5, PI-6, PI-7 and PI-8 whose numerals correspond with PAAs as shown in Table 3.1. PI-6 derived from OPDA showed the IR peak assigned to C-O stretching of ether group at 1238 cm^{-1} [40] and PI-8 derived from DSDA showed the peaks assigned to asymmetric and symmetric S=O stretching at 1323 cm^{-1} and 1148 cm^{-1}, respectively. These results clearly indicated the formation of the expected PIs which are clear, flexible and tough.

The crystalline structures of PIs after imidization were investigated by X-ray diffraction (XRD) which showed in Figure 3.6. The XRD pattern of PI-1 and PI-2 derived from CBDA gave two main diffraction peaks, one centered about 6° (2θ) and another centered about 17° (2θ) overlappling with a broad amorphous halo, while other PIs showed no crystalline peaks. These results indicate PI-1 structures having two cyclobutanes and two phenylenes as well as imide rings in the main chain induce the partial crystallization. It the methyl ester side group is replaced into ethyl, crystallization degree became low from 30 % to 10% because of possible steric hindrance of bulky ethyl groups against crystalline packing. For PI-3 to PI-8, they showed broad peak attributed to amorphous region. The broad peak is due to the diffraction of poor intermolecular packing combined with amorphous region [41]. These results were confirmed that carbonyl, ether, and sulfone groups of dianhydride could be increased

the flexibility of backbone resulting in loose polymer chain packaging and aggregates. However, PI-3 and PI-4 derived from PMDA, they do not have enough rigid structure to provide the semicrystalline in XRD pattern.

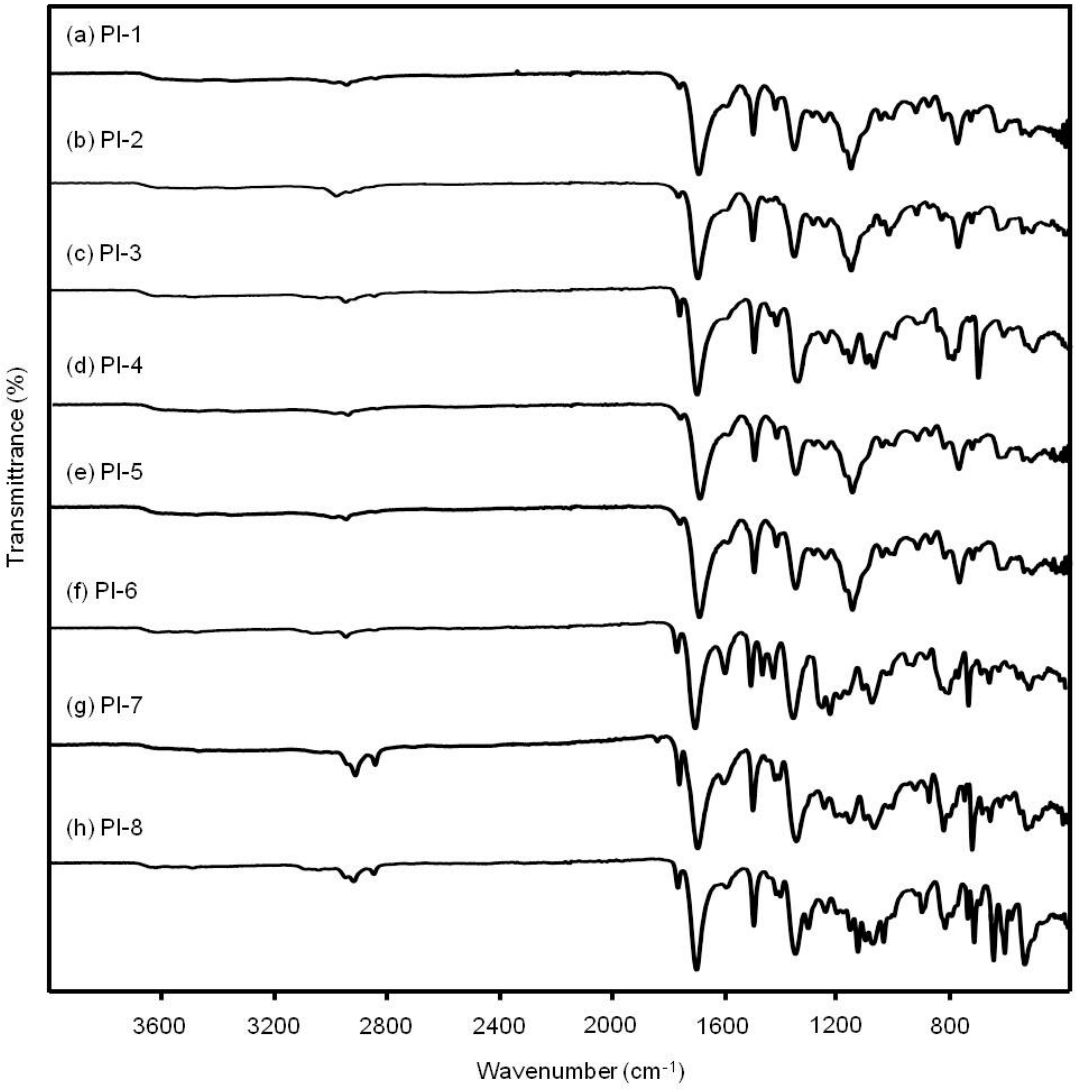

Figure 3.5 FTIR spectra of (a) PI-1 (b) PI-2 (c) PI-3, (d) PI-4 (e) PI-5 (f) PI-6 (g) PI-7 and (h) PI-8.

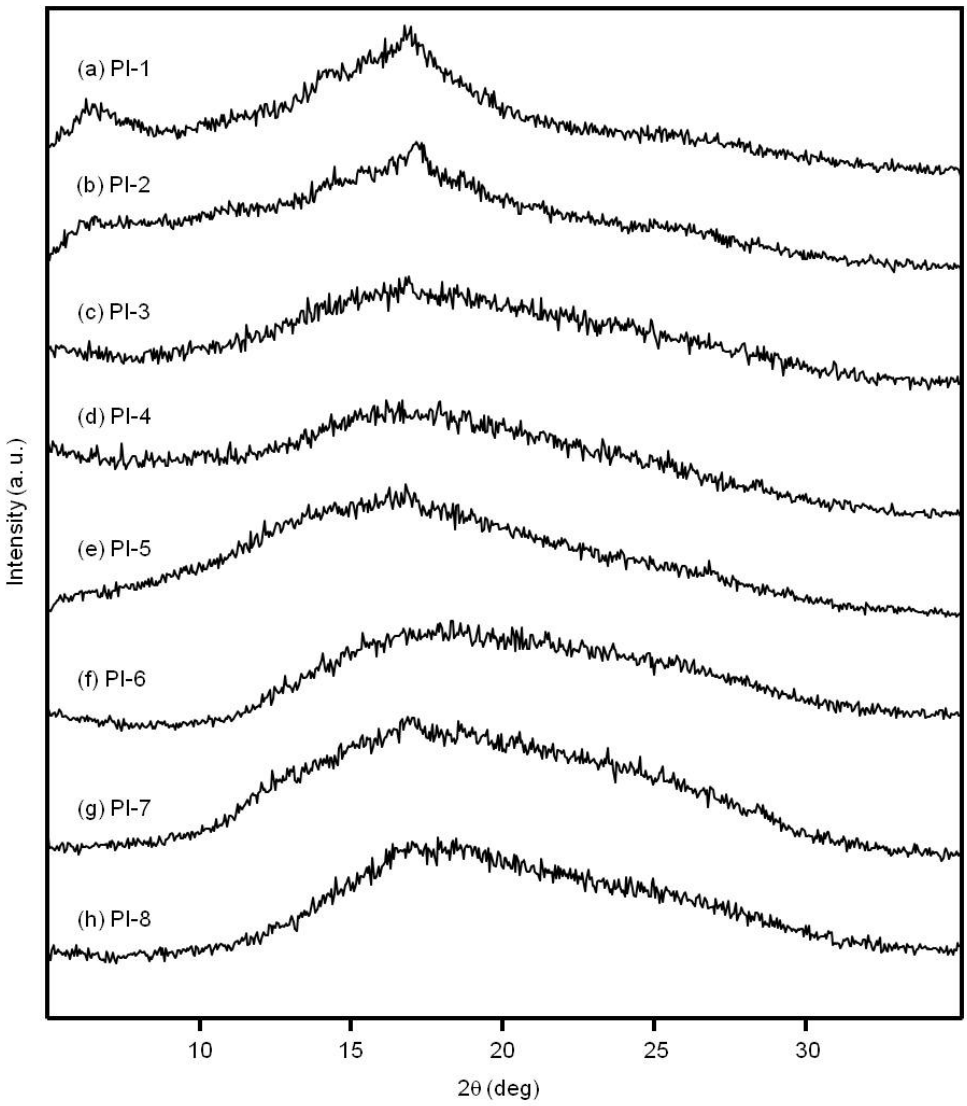

Figure 3.6 XRD profiles of (a) PI-1 (b) PI-2 (c) PI-3, (d) PI-4 (e) PI-5 (f) PI-6 (g) PI-7 and (h) PI-8.

3.3.2 Molecular weight and Viscosity of PAAs

The use of GPC to determine the weight-average molecular weight of (M_w), the number-average molecular weight (M_n) and the distribution of polymer molecular weight (PDI) of PAAs were showed in Table 3.1. The observation of the high molecular weight in the range of M_w ~ 2.09-3.99 × 10^5, M_n ~ 1.68-4.61 × 10^5 and M_w/M_n ~ 1.25-1.51 indicated that PAAs were successfully synthesized by polycondensation. The PAA

solutions have inherent viscosities of 0.34-1.23 dL/g at 30 °C, indicating moderate to high molecular weight of the polymers (Table 3.1). Although the inherent viscosity of PAA-6 was relatively low (0.34 dL/g) due to many flexible ether linkages, it also gave a self standing film probably because of the high molecular weight of polymer similarly to other PIs we prepared here. Fully bio-based PAA-1 derived from CBDA exhibited the highest molecular weight and the highest viscosity at 30 °C of all the PAAs shown here.

3.3.3 Density and Mechanical properties of PIs

Density and mechanical properties of PI films were summarized in Table 3.3. The clear, flexible and tough films were obtained by casting polymer solution in DMAc. In case of polymer's density which can be crucial factor in determining the application of polymer, all of PIs showed the density in the range of 1.15-1.31 $g.cm^{-3}$, which ranged lower than that of was Kapton^{TM} which was showed at 1.47 $g.cm^{-3}$ Because the steric effect of methyl- substituent or ethyl-substituent of 4ACA derivative part was an obstacle to the arrangement closely of polymer backbone, the weight per volume was low. In case of PI derived from 4,4′-oxydianiline (ODA) and CBDA, the density showed at 1.33 $g.cm^{-3}$ due to a good intra-molecular molecular packing of CBDA.

The mechanical properties of the PI films were measured by a tensile test. The PI films had tensile strength values in the range of 48-98 MPa, tensile modulus in the range of 4.2-13.4 GPa, and gross mechanical failure at strains in the range of 1.7-4.6 %. The tensile strength, tensile modulus, and mechanical failure of PI-6 were at 98 MPa, 13.4 GPa, and 4.5 %, respectively, which were indicated that the PI-6 film was the strongest and toughest.

Table 3.1 Inherent Viscosities, M_w, M_n, and PDI of PAAs and PIs.

Polymers	η_{inh} (dL/g)[a]	M_w[b]	M_n[b]	PDI[b]
PAA-1	1.23	3.99×10^5	2.78×10^5	1.43
PI-1	ND	ND	ND	ND
PAA-2	1.00	3.57×10^5	2.54×10^5	1.46
PI-2	ND	ND	ND	ND
PAA-3	0.50	3.19×10^5	4.61×10^5	1.45
PI-3	ND	ND	ND	ND
PAA-4	0.74	2.09×10^5	1.68×10^5	1.25
PI-4	ND	ND	ND	ND
PAA-5	0.72	3.06×10^5	2.25×10^5	1.36
PI-5	ND	ND	ND	ND
PAA-6	0.34	3.15×10^5	2.20×10^5	1.44
PI-6	ND	ND	ND	ND
PAA-7	0.53	2.56×10^5	1.70×10^5	1.51
PI-7	ND	ND	ND	ND
PAA-8	0.56	2.78×10^5	1.97×10^5	1.41
PI-8	ND	ND	ND	ND
Kapton™	ND	ND	ND	ND

[a] η_{inh}: Inherent viscosities measured with PAA at a concentration 0.5 dL/g in DMAc at 30 °C.

[b] M_w, M_n, PDI: The weight-average molecular weight, the number-average molecular weight and the distribution of polymer molecular weight of PAA using GPC.

ND: not determined

Another property, a more important aspect of density of polymer is the role it plays in calculating the specific strength and specific modulus. The specific strength is

simply the strength-to-weight ratio of polymer [42]. All of polymer showed high specific strength especially PI-6 that means the lightweight of polymers. In case of specific modulus, PI-6 also appeared the highest specific modulus values at 10.9 $Pa.kg^{-1}.m^{-3}$ suggested the high stiffness.

Table 3.2 Glass transition temperature, Crystalline degree, Degradation temperature and Density of the PIs.

Polymers	T_g (°C)[a]	Crystalline degree (%)[b]	Degradation temp.		Density ($g.cm^{-3}$)
			T_5(°C) [c]	T_{10}(°C) [c]	
PI-1	>350	30	365	390	1.20
PI-2	>350	11	380	395	1.26
PI-3	>350	0	410	425	1.15
PI-4	>350	0	380	395	1.21
PI-5	258	0	400	420	1.32
PI-6	248	0	395	410	1.23
PI-7	254	0	395	410	1.24
PI-8	275	0	410	425	1.31
Kapton™	>350	ND	557	574	1.47
ODA-CBDA[d]	>300	ND	425	454	1.33

[a] T_g: Glass transition temperature which was obtained from DSC at a heating rate of 10 °C/min in N_2.

[b] Crystallinity: % Crystallinity was obtained from XRD.

[c] T_5 , T_{10}: Temperature at 5% and 10% weight loss which was obtained from TGA at a heating rate of 10 °C/min in N_2.

[d] ODA-CBDA: PI derived from 4,4′-oxydianiline and 1,2,3,4-cyclobutane tetracarboxylic dianhydride as same preparation process as other PIs.

ND: not determined

Table 3.3 Tensile strength, Modulus, Elongation, Specific strength, Specific modulus and Refractive indice of PIs

Polymers	Tensile strength (MPa)[a]	Modulus (GPa)[a]	Elongation (%)[a]	Specific strength ($MPa.cm^3.g^{-1}$)[b]	Specific modulus ($GPa.cm^3.g^{-1}$)[b]	Refractive index[c]
PI-1	75	10.0	1.8	63	8.4	1.60
PI-2	81	4.3	2.1	64	3.4	1.65
PI-3	89	8.0	2.5	77	7.0	1.65
PI-4	96	5.7	4.6	79	4.7	1.65
PI-5	48	4.2	1.7	36	3.2	1.65
PI-6	98	13.4	4.5	80	10.9	1.64
PI-7	71	4.4	2.4	57	3.5	1.65
PI-8	90	4.8	3.3	69	3.6	1.64
Kapton™	63	2.8	12.8	43	1.9	1.65
ODA-CBDA[d]	ND	ND	ND	ND	ND	ND

[a] Tensile strength, Modulus and Elongation were obtained from tensometer at room temperature

[b] Specific strength and specific modulus were obtained from tensile strength/density and modulus/density, respectively.

[c] Refractive indices was obtained from Abbe refractometer.

[d] ODA-CBDA: PI derived from 4,4′-oxydianiline and 1,2,3,4-cyclobutane tetracarboxylic dianhydride as same preparation process as other PIs.

ND: not determined because of its brittleness.

3.3.4 Thermal properties

The thermal properties of these polymers were investigated by thermal gravimetric analysis (TGA) in a nitrogen atmosphere at a heating rate of 10 °C/min and the 5% and 10% weight loss temperature, T_5 and T_{10} were determined (Figure 3.7, Table

3.3). All these polymers exhibited good resistance thermal decomposition at 10 % up to 390-425 °C, especially PI-3 derived from PMDA exhibited the highest thermal stability at 10% weight loss temperature up to 425 °C. This result indicated that high resonance energy of the benzene rings due to delocalization of π-electrons and the great number of resonance structures. Moreover, the strength of imide bonds, resulting from the competitive π-n conjugation between carbonyl group and the non pair electron couple from the nitrogen atoms as well as from the conformation state of 5-member ring could be increased degradation temperature. Nevertheless, PI-4 also derived from one aromatic ring of PMDA was not governed the thermal stability over 400 °C. It was due to the steric effect of ethyl groups in the structure. In case of PI-1 and PI-2 derived from cyclobutane dianhydride showed lower degradation temperature than 400 °C owing to no delocalization of π-electrons in diamine parts.

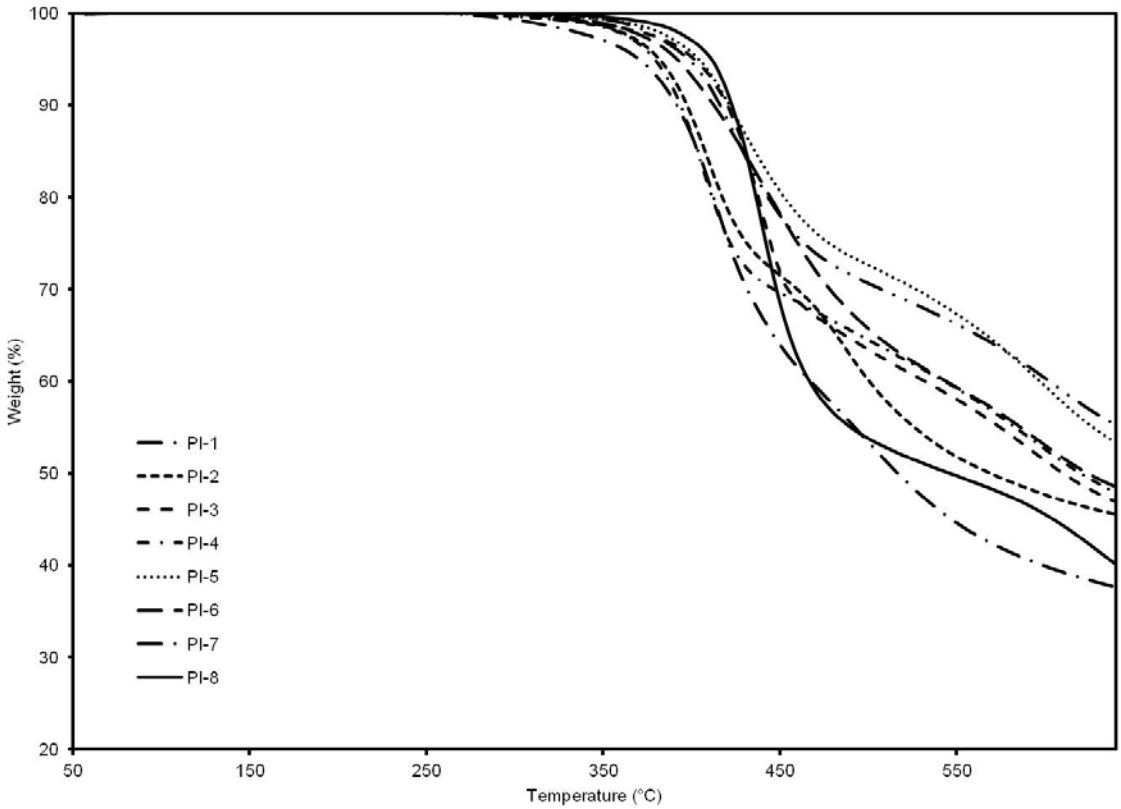

Figure 3.7 TGA curves of PI films (under a nitrogen atmosphere, 10 °C/min).

T_g values of the PIs were determined by differential scanning calorimetry (DSC) under a nitrogen atmosphere (Figure 3.8, Table 3.3). PI-5, PI-6, PI-7 and PI-8 showed T_g values at 260 °C, 250 °C, 240 °C and 275 °C, respectively. We expected, the T_g values of these PIs both depended on the structure of the dianhydride component and decreased with increasing flexibility of PI backbone [25, 40]. PI-1 to PI-4 exhibited no T_g below 350 °C whis is measuring limitation of DSC machaine, meaning ultra-high T_g owing to their rigidity and symmetric structure. Semicrystallinity and symmetry would be increased uniform structure of PIs, resulting too high T_g. Although the sulfone group of DSDA should give the flexibility of PI-8 backbone, the PI had a higher T_g than PI-5, PI-6 or PI-7. It should be conjectured that an intermolecular charge transfer complex (CTC) of electron-rich diamine phenylene with electron-poor dianhydride phenylene

connecting with sulfone induces the good interchain packing in PI-8. Relatively higher T_g of others may be also attributed to interchain CTC of electron-rich diamine phenylene with electron-poor dianhydride phenylene connecting with ketone. Overall the T_g values of any PIs prepared here were much higher than those of conventional bio-based polymers of poly(lactic acid)s, polyamide-11, and other aromatic bio-based polymers reported thus far. The stability of planar 5-membered ring of imide linkage resulting from π-π conjugation between carbonyl group with nitrogen atom without lone electron pair could increase T_g. Such high T_g property was suitable to apply for super-engineering plastics.

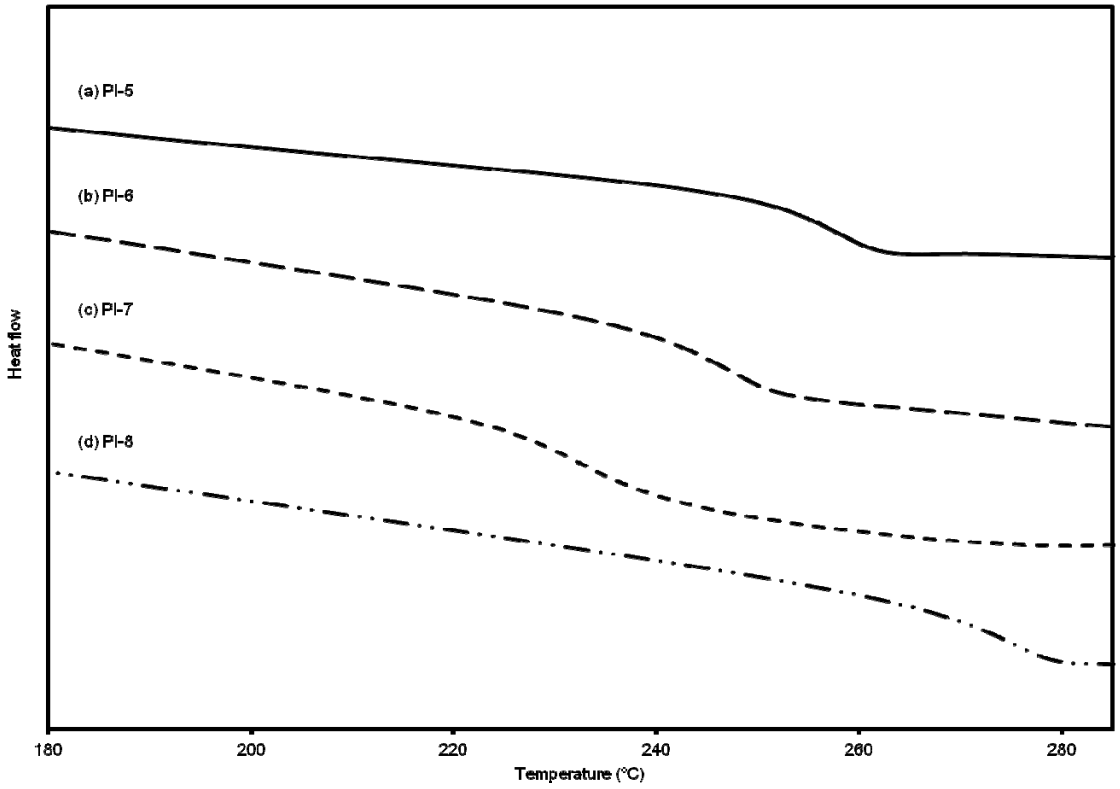

Figure 3.8 DSC curves of PI films (under a nitrogen atmosphere, 10 °C/min).

3.3.5 Refractive indices

Refractive indices of PI films ranged from 1.60-1.65 as listed in Table 3.4. The high refractive indices are primarily due to the relatively dense molecular packing originating from the rigid structure composed of aromatic groups with high electron density, comparing to other transparent plastics such as polycarbonate (1.58) and poly(ethylene terephthalate) (1.57-1.58). Lower refractive indices of PI-1 and PI-2 derived from aliphatic CBDA dianhydrides than other PIs were due to lack of aromatic moiety in dianhydride.

3.4 Conclusion

Bio-based aromatic diamines 4,4′-diamino-α-truxilic acid was prepared as a photodimer of 4-aminocinnamic acid which was bioavailable from genetically-manipulated *Escherichia coli* although direct biosynthesis of aromatic diamines has never been reported. 4,4′-diamino-α-truxilic acid reacted with various anhydrides to create the poly(amic acid) and then the successive heat treatment gave the polyimides (PI). When we use 1,2,3,4-cyclobutane tetracarboxylic dianhydrides (CBDA) as a counter monomer, the polyimides were fully bio-based because CBDA is also a photodimer of biomolecular maleic acid derivatives. All the bio-based PI films we prepared here showed ultrahigh thermal resistance of T_g over 350 ^oC which is the highest value of all the bio-based plastics reported as far as we know. The PI films additionally showed high tensile strength and high Young's modulus and high refractive indices may lead to development of super-engineering materials.

CHAPTER 4

HIGH PERFORMANCE BIO-BASED POLYIMIDES DERIVED FROM 4-AMINOCINNAMATE BIOCHEMICALS WITH THEIR SURFACE ENERGY FOR BIOMEDICAL APPLICATION AND THEIR DEGRADABILITY

CHAPTER 4

HIGH PERFORMANCE BIO-BASED POLYIMIDES DERIVED FROM 4-AMINOCINNAMATE BIOCHEMICALS WITH THEIR SURFACE ENERGY FOR BIOMEDICAL APPLICATION AND THEIR DEGRADABILITY

4.1 Introduction

Polymeric materials have recently been established as having great potential for several applications in the biomedical field such as bone plates and joint replacement implants [43], bone cements [44], drug delivery systems [45, 46] and tissue engineering scaffolds [47, 48]. Because their low specific weight, high mechanical strength, toughness and chemical resistance and hence stability, utilization of polymer is preferred over metals and ceramics. Metals are known for high strength, ductility, and resistance to wear. Shortcomings of many metals include low biocompatibility, corrosion, too high stiffness compared to tissues, high density, and release of metal ions which may cause allergic tissue reactions [49]. Ceramics are known for their good biocompatibility, corrosion resistance, and high compression resistance. Drawbacks of ceramics include, brittleness, low fracture strength, difficult to fabricate, low mechanical reliability, lack of resilience, and high density [50]. Conventional polymers have been used in biomedical fields such as poly(vinyl chloride), polyethylene (PE), poly(methyl methacrylate), segmented polyetherurethane (SPU), poly(dimethyl siloxane), polytetrafluoroethylene, cellulose, etc [51]. Synthetic biocompatible polymeric materials which engineer to interact with biological systems were provided the significant advantage of being able to be used as biomaterials for modern medical application [52]. They must be biocompatible meaning that the ability of material to

perform the appropriate specific function with host response and structural compatibility which is the optimal adaptation to mechanical behavior of implant within body [50, 53]. An aromatic polyimide (PI) is one of the most vital classes of high performance polymer with their excellent thermal, superior chemical stability, high radiation resistance, good mechanical properties and low dielectric constant [37]. They can be used as super-engineering plastics in a wide scope of application including variety modern industrial and commercial applications such as in electronic industry, adhesive, laminating resin, film or coating and aerospace [1]. Factors that contribute PI to high performance polymers are presented such as resonance stabilization, molecular symmetry, high molecular weight and high molecular distribution, rigid intrachain structure, mechanism of bond cleavage and additives or reinforcements (fillers, clays, miscellaneous nanoparticles) [39]. Furthermore, they are the best candidates for high refractive index polymer with high transparency because of their high polarizable molecular chains and high aromatic contents [54]. Another property of them is low coefficient of thermal expansion in organic compound; few errors from expansion with used at high temperature and also readily shaped and machined which was suitable for use in wider processibility window [38]. Therefore, PI hold an important position in the field of medicine as structure materials implanted in the body and as surgical aids. There are known PIs, for example, Kapton^{TM}, is used as flexible substrate in neuroprosthesis devices for functionally interfacing parts of the nervous system. The micro-implant is used to stimulate parts and structures of neurological disorder with the aim of implanted electrical circuitry or record the electrical activity of nerve cells [55]. Although it was proved to be biocompatible with the human body, it is not used in mechanical load bearing application. A number of researchers have suggested using

Vespel® as a possible bearing material for orthopedic use [56]. It has the same density and same modulus as bone and has good elasticity and damping of shock forces. However, toxicological aspects have never tested and it likely to undergo hydrolysis in the body, especially under wear and friction conditions. Among the known PIs, this research focused on it prepared from biological molecule that no bio-derived PI was previously reported. Bio-derived PIs are of utmost interest since these biomaterials tend to be broken down and excreted or resorbed without removal or surgical revision. Nevertheless, many key properties must be concerned, for examples, (1) have appropriate mechanical and thermal properties (2) possess a high optical transparency and a high refractive index; and (3) include non-toxic and biocompatible for medical application to overcome the shortcoming of conventional PI.

Here, we tried to describe new concept of the synthesis of aromatic diamine monomers from bio-derived 4ACA. However bio-derived PI were very difficult to prepare since the aromatic diamines cannot be made using biosynthesis as they are seriously incompatible with microorganism or plant cells, presumably because of the combined interaction of ionic, hydrophobic, and π-electron-related factors with cell constituents. Even aromatic monoamines have rarely been produced by microorganism [57, 58, 59]. Photochemical dimerization of 4ACA conduce the formation of new dimers by the reaction of two unsaturated 4ACA. New aromatic diamine was used for PIs syntheses as following. PI from aromatic diamines were synthesized with tetracarboxylic dianhydride, such as, 1,2,3,4-cyclobutane tetracarboxylic dianhydride (CBDA), pyromellitic dianhydride (PMDA), 3,3',4,4'-benzophenone tetracarboxylic dianhydride (BTDA), 4,4'-oxydiphthalic anhydride (OPDA), 3,4,3',4'-biphenyltetracarboxylic dianhydride (BPDA) and 3,3',4,4'-diphenylsulfone

tetracarboxylic dianhydride (DSDA) by using polycondensation procedure. The variation in the structure of aromatic diamines and dianhydrides had a dramatically effect on the properties of PI like T_g and T_m toward understanding these structure-property relationships. The resulting PIs were flexible polymer with high performance properties which is high heat resistance, good mechanical property, chemical inertness, excellent transmissibility and high refractive indices. Considering the above property, there appear to be a great need for various medical applications. Flexible PIs with high optical properties and refractive indices are able to use in intraocular retinal prosthesis implanted in eyes instead of conventional PIs that have high refractive indices but poor transparency. PIs with high mechanical strength can be proposed for several orthopedic applications. Additionally, the biocompatible and non-toxic PI was necessary properties of bio-medical polymer to open the door to develop high performance materials with varied cell adhesion behavior. Finally, degradable properties which have received increasing attention were studied to develop durable polymers from bio-based monomer for creating a long term carbon stock.

4.2 Experimental Section

4.2.1 Materials

All of materials were used as same type as chapter 4.

4.2.2 Optical properties

PAA solutions were dissolved in DMAc and were cast onto quartz cell with thickness about 9-15 μm. All of obtained PAA films were further stepwise increased temperature to become PI films with the same method as previous section. Ultraviolet-

visible (UV-Vis) spectrophotometer (Perkin Elmer, Lambda 25 UV/Vis spectrophotometer) was used to measure film transparency at room temperature in the 200-800 nm spectral regions.

4.2.3 Solubility test

The solubility of polymers was investigated as 0.001 g of polymeric sample in 1 mL of various organic solvent at room temperature and at 60 °C.

4.2.4 Contact angle Measurements and surface free energy estimation

The surface wettability and the hydrophobic properties of the polymers were assessed by static contact angle (θ) measurements using the sessile drop method. Three different liquids were used: ultra-pure water (polar), ethylene glycol and diiodomethane (non-polar). The contact angle between a droplet (1μL) of liquid and polymer surfaces were measured by using contact angle measurement apparatus (Drop-Master DM 300, Kyowa Interface Science Co). Total surface energies and their dispersion, polar and hydrogen bonding components were calculated using the equation as following. The presented data are the average of three measurements at different locations on the film surface.

$$\gamma^{tot} = \gamma^{LW} + 2\sqrt{\gamma^{+}\gamma^{-}} \quad \ldots\ldots\ldots\ldots (1)$$

where γ^{LW} is surface energy from van der Waals interaction or dipersion, γ^{+} is surface energy from acceptor interaction, γ^{-} is surface energy from donor interaction and γ^{tot} is total surface energies.

4.2.5 In Vitro Cell culture

Cell culture A mouse fibroblast-like cell line (L929) was selected for all the biological assays in order to evaluate the effect of varied PIs on cell adhesion. The L929 fibroblast cell line was obtained from the American Type culture collection (Manassa, VA, USA). The cells were cultured in Dulbecco's Modified Eagle's Medium (DMEM, Sigma-Aldrich, USA), supplemented with 10% of heating inactivated fetal bovine serum (FBS, Biochrom AG, Germany) incubated at 37 °C in humidified atmosphere with 5% of CO_2.

Cell adhesion Polymer films were casted on 15 mm micro cover glass, seeded with 100 μL of a cell suspension (2.5×10^4 cells.mL^{-1}) and cultured for 1, 2 and 4 day at 37 °C in 24-well multiplates. Prior to culturing, all the polymers were sterilized with ethanol. Well plate was used as controls. After each incubation period, the samples were rinsed with a buffer saline (PBS, Sigma-Aldrich, USA). We can distinguish whether the cells change from a circular to an elongated shape after adhesion [60]. The number of cells adhering to the surface of polymers was counted with trypan blue staining on a hemocytometer.

4.2.6 Degradability and Durability

4.2.6.1 Degradation of PAA, imidized PAA at 150 °C and PI solutions by UV irradiation

From photo cleavage of PAAs, partial imidized PAAs at 150 °C, and PIs, UV irradiation was carried out on a Xe lamp (300 W, Asahi Spectra Co. Ltd.; MAX-303) equipped with 254 nm band-pass filter.

^{1}H Nuclear magnetic resonance (NMR) spectroscopic analysis The ^{1}H NMR spectra were obtained by a Bruker Biospin AG 400 MHz, 54 mm spectrometer using DMSO-d_6 and trifluoroacetic acid-*d* as the solvent at concentration 10 mg/mL.

Gel permeation chromatography (GPC) The polymer molecular weight distribution was determined by gel permeation chromatography (GPC) equipped with a UV and refractive index detector (2075 Intelligent UV/Vis detector, JASCO and PU-2080 Intelligent HPLC Plus, JASCO). The dried samples were dissolved in dimethylformamide at a concentration 5 g/L and eluent through the column at a flow rate of 0.5 ml/min at 40 °C. Pullulan standards (Shodex GPC KF-801 and KF-802) were used to obtain a primary calibration curve.

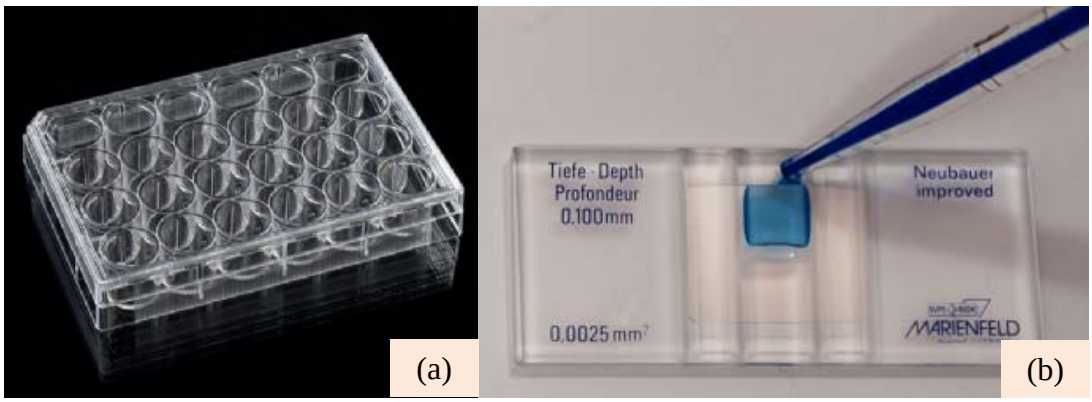

Figure 4.1 (a) 24-well multiplate for cell culture and (b) hemocytometer with the volume of 0.025×0.025×0.100 mm^3 for counting cells.

4.2.6.2 Durability of PI films

Durability in an environment PI films with circle shape (diameter = 0.6 mm) were buried 20 cm in soil (in JAIST, Nomi, Ishikawa, Japan), under the condition from

the nature such as light, rain, bacteria and moisture. The soil dispersion with 0.1 $g.ml^{-1}$ concentration showed pH = 5.2. The polymer films were removed after 4 months, brushed softly, washed with distilled water several times and dried under vacuum to constant weight. The degree of degradation was evaluated as the weight loss normalized with respect to the initial surface area [61].

Degradation of PI films in tensile properties of UV irradiation Irradiation was carried out for the specimens shaped in dumbbell by UV irradiation. Radiation damage was evaluated by measuring tensile properties. The tensile measurements such as tensile strength, breaking elongation and tensile modulus were carried out on a tensometer, instron 3365-L5 at room temperature. The maximum load was 5 kN, and the elongation speed was 0.5 $mm.min^{-1}$.

4.3 Result and Discussion

4.3.1 Optical properties

Figure 4.2 showed the UV-Vis transmission spectra of PAA and PI films on the wavelength, where the curves were normalized to the transmittance of the film with a thickness of 9-15 μm. Optical transparency at 450 nm (T_{450}) and the cutoff wavelengths (λ_0) of UV-Vis spectra are summarized in Table 4.1. The PAA films showed no color or pale-yellow colors and T_{450} values of most polymers were 88-100 %. After imidization, the films became darker yellow and showed lower T_{450} values. PI-1, PI-2, PI-3 and PI-5 kept high transparency of 79-88 % while PI-4, PI-6, PI-7 and PI-8 showed T_{450} range of 65-69 % but is much more transparent than commercial Kapton^{TM}. The imidization caused ring-closing reactions making more efficient charge transfer between benzene

from diamines and one from dianhydrides leading to the color change [62]. Kapton™ has strong dark brown color due to the characteristic absorption tailing from UV to visible region, caused by strong charge transfer (CT) interaction in electron-rich oxydianiline component with dianhydride moieties. The much higher optical transparency of the present PAAs and PIs than that of Kapton™ should be owing to cyclobutane moiety in diamine component which has less electron-rich benzenes to weaker CT interaction with dianhydride component than oxydianiline in Kapton™. In almost colorless PI-1 and PI-2 films derived from CBDA which is one of the most simple alicyclic dianhydride monomers, non-conjugated aromatic structures in dianhydride component gave a weak electron accepting ability to imide moieties [63].

In addition, aliphatic dianhydrides of PAAs exhibited higher λ_0 and less yellow than PIs (Table 4.1). The longest λ_0 and highest transmittance of PI-3 indicated to the optical transparency of polymers determined by electronic structure (π electrons) of an aromatic ring, whereas the intermolecular interactions do not expose an important influence.

Table 4.1 λ_0 and T_{450nm} of PAAs and PIs

Polymers	λ_0 (nm)[c]	T_{450nm} (%)[c]
PAA-1	284	99.51
PI-1	270	88.24
PAA-2	290	96.94
PI-2	282	86.86
PAA-3	345	95.73
PI-3	357	80.05
PAA-4	329	91.78
PI-4	355	50.69
PAA-5	329	96.86
PI-5	326	79.09
PAA-6	326	87.94
PI-6	363	68.92
PAA-7	351	89.47
PI-7	383	65.35
PAA-8	346	90.07
PI-8	366	82.18
Kapton™	384	0.70

λ_0, T_{450nm}: UV cutoff wavelength and transmittance at 450 nm using UV/Vis spectrophotometer.

(a)

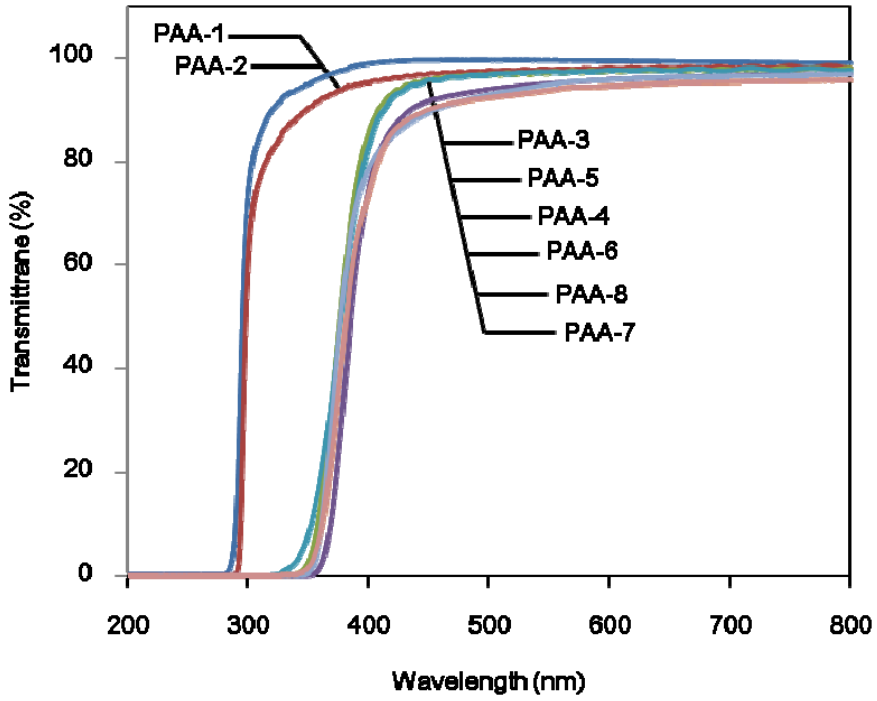

(b)

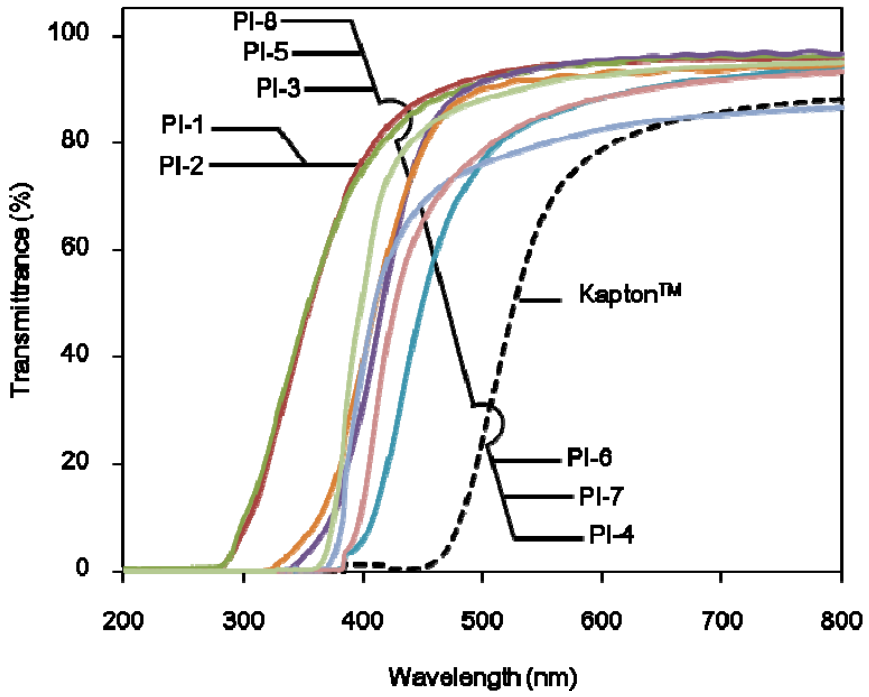

Figure 4.2 UV-Vis spectra of (a) PAAs (b) PIs and Kapton™ film (thickness ~9-15 μm).

4.3.2 Solubility test

As listed in the table 4.2, all of PIs were insoluble in all of solvents even by heating except conc. sulfuric acid, probably due to theirs coplanar ring of aromatic-imide structure. Nevertheless, PAAs were soluble in polar aprotic solvent, for example, NMP, DMAc, DMF and DMSO and polar protic solvent, such as, conc. sulfuric acid at room temperature. These results could be confirmed that PIs have high chemical resistance.

Table 4.2 Solubility behavior of PAAs and PIs

Polymers	Solvents								
	H_2O	MeOH	EtOH	$(CH_3)_2CO$	CH_3CN	DMF	NMP	DMAc	DMSO
PAA-1	–	–	–	–	–	+	+	+	+
PI-1	–	–	–	–	–	–	–	–	–
PAA-2	–	–	–	–	–	+	+	+	+
PI-2	–	–	–	–	–	–	–	–	–
PAA-3	–	–	–	–	–	+	+	+	+
PI-3	–	–	–	–	–	–	–	–	–
PAA-4	–	–	–	–	–	+	+	+	+
PI-4	–	–	–	–	–	–	–	–	–
PAA-5	–	–	–	–	–	+	+	+	+
PI-5	–	–	–	–	–	–	–	–	–
PAA-6	–	–	–	–	–	–	+	+	+
PI-6	–	–	–	–	–	–	–	–	–
PAA-7	–	–	–	–	–	+	+	+	+
PI-7	–	–	–	–	–	–	–	–	–
PAA-8	–	–	–	–	–	+	+	+	+
PI-8	–	–	–	–	–	–	–	–	–

Polymers	Solvent							
	Toluene	Hexane	THF	$CHCl_3$	$(C_2H_5)_2O$	CH_2Cl_2	EtOAc	Conc. H_2SO_4
PAA-1	–	–	–	–	–	–	–	+
PI-1	–	–	–	–	–	–	–	+
PAA-2	–	–	–	–	–	–	–	+
PI-2	–	–	–	–	–	–	–	+
PAA-3	–	–	–	–	–	–	–	+
PI-3	–	–	–	–	–	–	–	+
PAA-4	–	–	–	–	–	–	–	+
PI-4	–	–	–	–	–	–	–	+
PAA-5	–	–	–	–	–	–	–	+
PI-5	–	–	–	–	–	–	–	±
PAA-6	–	–	–	–	–	–	–	+
PI-6	–	–	–	–	–	–	–	+
PAA-7	–	–	–	–	–	–	–	+
PI-7	–	–	–	–	–	–	–	+
PAA-8	–	–	–	–	–	–	–	+
PI-8	–	–	–	–	–	–	–	+

+:Soluble at room temperature, ±: Partially soluble at 60 °C, –: Insoluble at 60 °C

$(CH_3)_2CO$ is acetone, CH_3CN is acetonitrile, $CHCl_3$ is chloroform, $(C_2H_5)_2O$ is diethyl ether, THF is tetrahydrofuran, CH_2Cl_2 is dichloromethane, EtOAc is ethylacetate

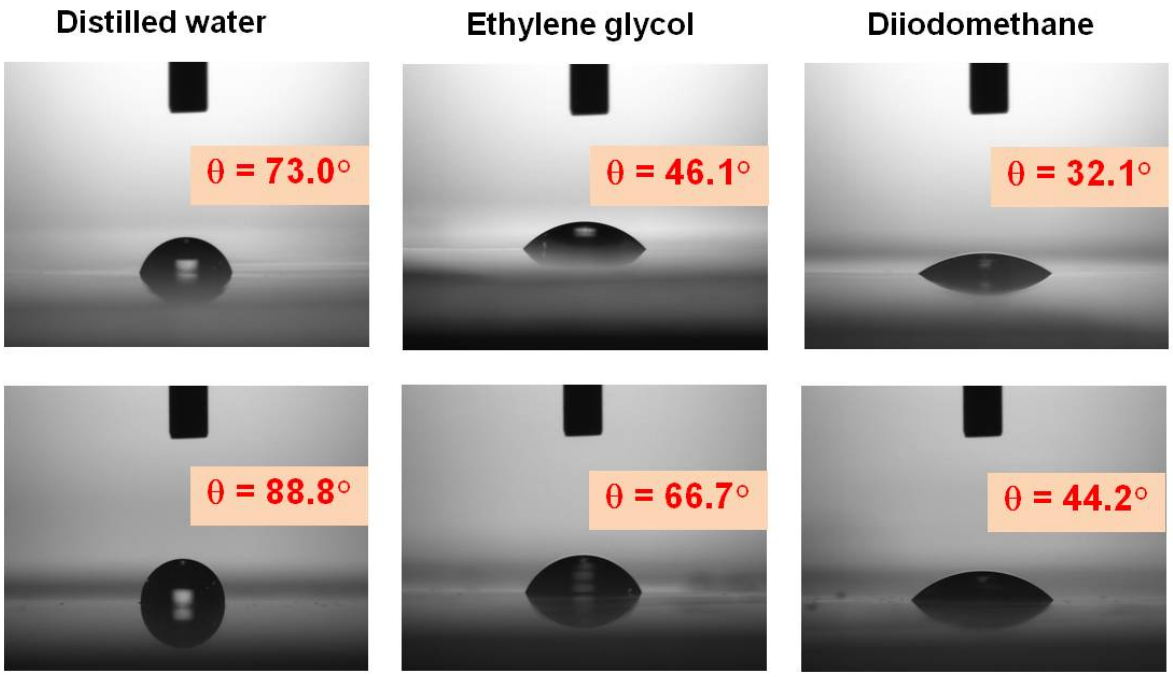

Figure 4.3 Contact angle images of (a) Kapton^{TM} and (b) PI-5 film.

4.3.3 Contact angle and Surface energy

Contact angles were measured on all PIs using the three test liquids: water, ethylene glycol and diiodomethane with the sessile drop technique (Table 4.3). Contact angle images of PI-5 film were used as representative of all PIs compared with Kapton^{TM} (Figure 4.3). In general, dispersive component (non-polar) and donor/acceptor component (polar) have a great influence on contact angle [64]. Contact angle measurement, especially for water, increased with the increase of treatment temperatures, indicating that the surface of the PI films became less polarity or high hydrophobicity (~80°-88°). Moreover, they had a slightly larger dispersive component (γ^{LW}) and a slightly smaller non-dispersive component (γ^{+} and γ^{-}). Therefore, van der waals force played a crucial role for PI films. PI-5, PI-6, PI-7 and PI-8 having two benzene rings in dianhydride component in the repeated unit showed higher contact

angle in water (~86°-88°) while PI-3 and PI-4 having only one showed lower contact angle (~80°-85°). However, PI-1 and PI-2 containing no benzene ring in dianhydride component exhibited higher contact angle in water than PI-3 and PI-4, presumably due to less polarity of dianhydride cyclobutane rings. Furthermore, all of PI films may be considered as monopolar basic owing to their zero values of basic component (γ^+) < 0.3 $mJ.m^{-2}$.

Table 4.3 Contact angle (°) and surface free energy ($mJ.m^{-2}$) of PI films.

Polymers	Contact angles (°)			Surface energy ($mJ.m^{-2}$)			
	D.I.	E.G.	M. I.	γ^{LW}	γ^+	γ^-	γ^{tot}
PI-1	85.53	57.67	48.87	34.902	0.111	3.899	36.218
PI-2	85.93	64.77	40.43	39.393	0.166	5.399	41.284
PI-3	80.36	62.37	42.26	38.452	0.131	9.258	40.652
PI-4	81.43	64.37	37.93	40.636	0.355	8.903	44.189
PI-5	88.83	66.67	44.2	37.437	0.108	4.107	38.768
PI-6	85.20	64.70	44.00	37.543	0.098	6.049	39.084
PI-7	86.46	70.30	59.56	28.825	0.010	7.777	29.384
PI-8	86.17	67.67	54.37	31.807	0.016	6.760	32.456
Kapton™	73.00	32.10	46.10	43.320	0.020	9.600	44.135

D.I. is distillated water.

E.G. is ethylene glycol.

M.I. is iiodomethane.

γ^{LW} is dispersive component of surface energy (non-polar).

γ^+, γ^- is non-dispersive component of surface energy which is electron accepting component (polar) and electron donating component (polar).

γ^{tot} is total surface energy of materials.

4.3.4 Cell culture

The adhesion and proliferation of the L929 cell cultured on various PI film surfaces were shown in Figure 4.4. Several properties have been proposed to influence cell behavior in culture. These include surface charge, topography, hydrophobicity or hydrophilicity, surface chemistry and surface energy [65]. It is generally accepted nowadays that the adhesion and spreading of cells on polymer surfaces, is related to the polar and dispersion components of surface free energy. Particularly, cells were believed to generally adsorb on moderate hydrophilic surface (~57°) compared with a hydrophobic surface, regardless of the cell type used, which was mainly attributed to approximately hydrophilic interaction between cultured cell and the surface [65]. Commercial Kapton^{TM} was used as a positive control because good cell compatibility of Kapton^{TM} has already been accepted [66]. At the first day and second day of growth, the number of adhered cells did not increase, but the number increased at the 4th day of growth. All the PI films showed not very large difference in cell number and exhibited good cell compatibility although Kapton^{TM} showed slightly higher number of cells adhered than these PI films.

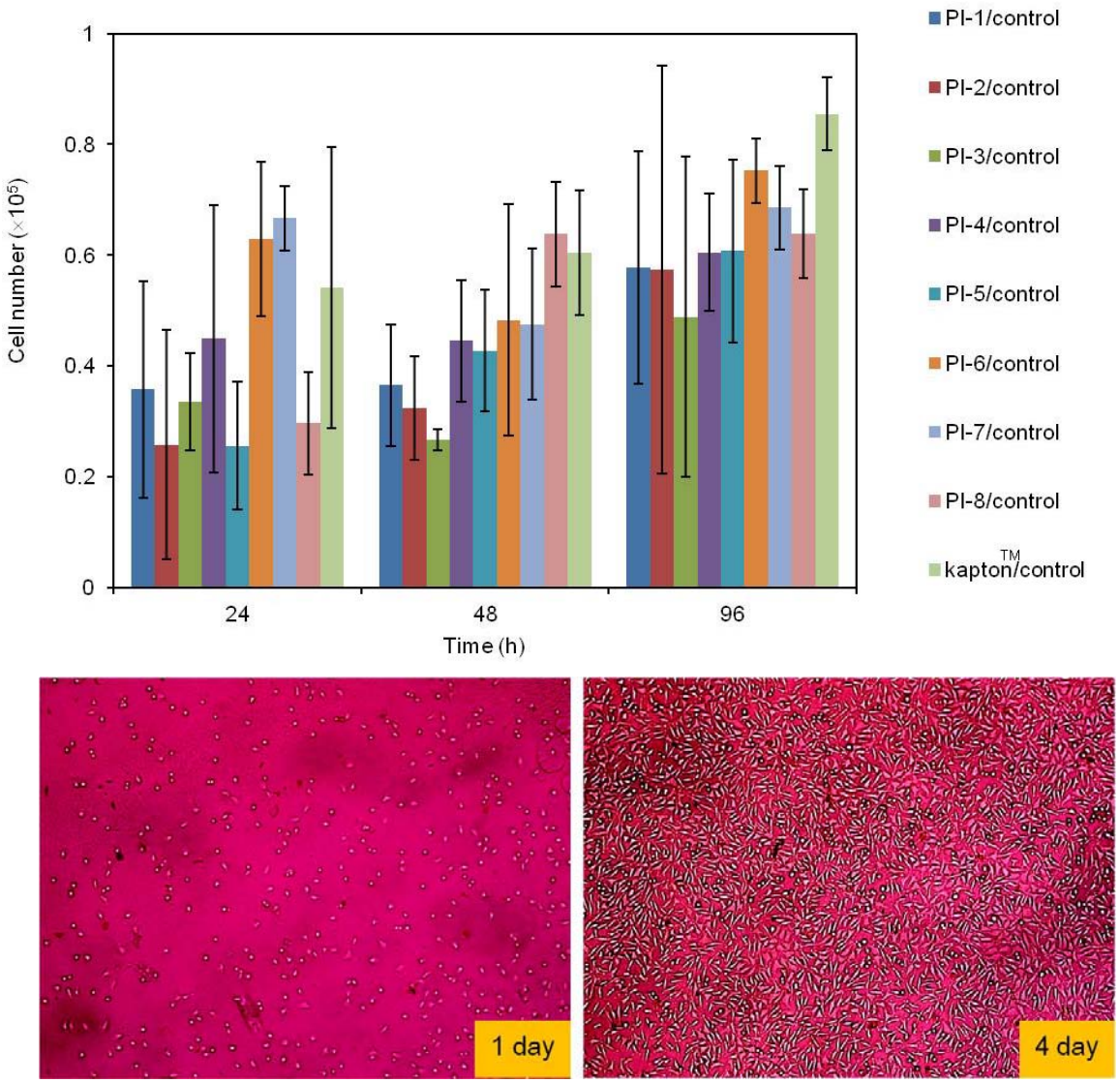

Figure 4.4 (a) L929 fibroblasts after different time periods in contact with PIs and (b) PI-6 as PI representative at the first and the 4th day of cell growth.

4.3.5 Degradability and Durability

Degradability of PAA, imidized PAA at 150 °C and PI solutions by UV irradiation

The effects of UV conversion into monomer is an important feature for bio-based polymers to secure long term carbon fixation because of the prolongation of the

the life-span of the material by chemical recycling. The present PIs had good thermal stability and mechanical performance as mentioned on chapter 3. In addition, the polymer backbone had a chemically stable aromatic ring and imide bond. Therefore, it is thought that typical hydration methods such as biodegradation would not be effective.

Therefore, I tried to establish a UV degradation focusing on cyclobutane moieties. If the degradation proceeded as planned, derivatives of vinyl bond of cinnamate will be occurred. PAA fibrils, imidized PAA films at 150 °C and PI films in solution state were used as the representative of UV degradability. PAA fibrils and imidized PAA films were dissolved in DMSO-d_6 while PI films were not dissolved in DMSO-d_6, TFA-*d* was used. If PAAs showed their high durability against UV, PIs will show higher durability due to their strong ring closing of dianhydride component in polymer backbone. The initial compound in this research, cinnamate, was irradiated by UV to cleavage cyclobutane ring of PAAs. The ^{1}H NMR spectra of PAA-1 solution as representative under UV irradiation (Figure 4.5) showed vinyl proton in the range of 5.66-6.96 ppm and cleavage of cyclobutane ring, especially from dianhydride in the range of 3.57-3.71 ppm of recovered cinnamate. PAA-1 and PAA-2 displayed 19.81 % and 25.00 % degradation under 72 hours UV irradiation. GPC of PAA-1 and PAA-2 after irradiation for 72 hours showed a peak at a maximum of M_n and M_w range of 0.51-0.70 $\times$ 10^4 and 0.77-1.19 $\times$ 10^4, respectively, and PDI ranged 1.50-1.69. This result indicates that the molecular weight loss was due to UV degradation.

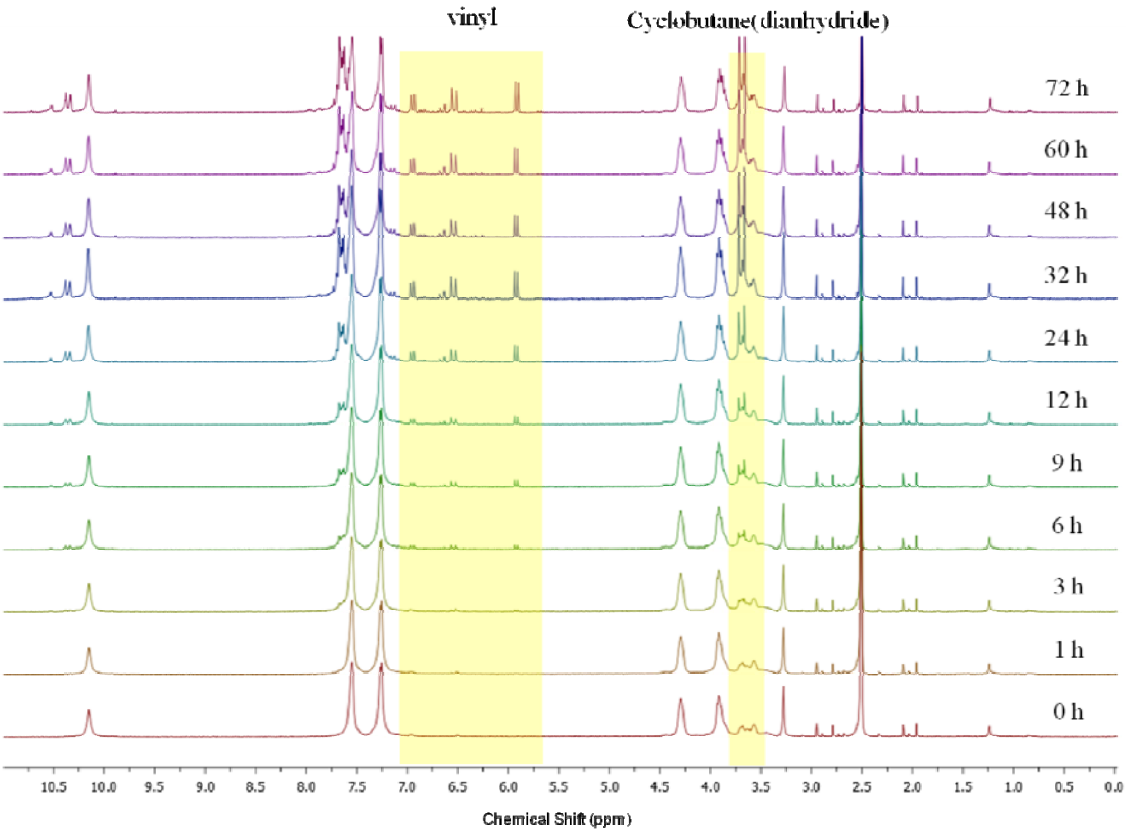

Figure 4.5 Durability of PAA-1 solution under UV irradiation with various hours by ^{1}H NMR measurement.

Durability of PI films in an environment and under UV light

PI films that had been buried in soil for 4 months (Figure 4.6) did not show deformation or weight loss. These findings indicate environmental durability of PI films; not only by rainwater or moisture but also by microbial action.

In case of PI film under UV light for 10 days, PI-1 film was used as representative. The physical properties of PI-1 also was not change, film still strong and has tensile strength as same values as before UV irradiation at about 75 MPa.

Figure 4.6 Physical appearances of PI films before burring in soil for degradation behavior in an environment under light, rainwater, moisture and bacteria.

Therefore, high durable PIs against hydrolysis and UV light were developed to respond to the concept of durable materials which are able to be long carbon stock. However, these high durable PIs can recycle by dissolve in TFA and then UV irradiation to cleavage cyclobutane backbone. They could be had high-performance properties under lifetime to widely applied in manufacture of automobile parts, electronic devices including biomedical applications and can be degraded after using within a specific condition.

4.4 Conclusion

Bio-based high performance PIs showed excellent transparency, especially PI-1 and PI-2 containing 1,2,3,4-cyclobutane tetracarboxylic dianhydrides (CBDA) as a counter monomer. The PI films additionally showed high chemical resistance due to their coplanar ring of aromatic-imide structure. These characteristics of bio-based PIs such as good thermal property, high tensile strength strength, high Young's modulus as mentioned on chapter 3 including excellent transparency and high chemical resistance can lead to development of high-performance materials we will be able to use very safely in biomedical applications owing to good cell adhesion. They may lead to develop opthalmological materials because of their excellent transparency and high refractive indices.

CHAPTER 5

CONCLUSION REMARKS

CHAPTER 5
CONCLUSION REMARKS

The research in this thesis focused on the syntheses of high performance bio-based polymer including polyamide and polyimides (PIs) derived from 4-aminocinnamate biomonomer. The development of these high performance bio-based polymers was crucial to establish sustainable low-carbon society. The important and interesting results throughout this study are summarized as follows.

In **Chapter 2**, bio-based aromatic diamine 4,4′-diamino-α-truxillic acid was successfully prepared as a photodimer of 4-aminocinnamic acid, bioavailable from genetically-manipulated *Escherichia coli*, even though the direct biosynthesis of aromatic diamines has never been reported. Photo-irradiation was a good synthesis method because it can be accurately targeted and highly selective. The single crystal of 4,4'-diamino-α-truxillic acid dihydrochloride was used to confirm the *trans*-stereoisomer product after UV irradiation. It also indicated that 4,4'-diamino-α-truxillic acid dihydrochloride had high purity because small needles of crystal was able to be prepared. The polyamide was prepared from 4,4'-diamino-α-truxillic acid methylester and dipicolic acid, both bioavailable compounds. The relationship of its molecular structure and properties was clarified. The polyamide showed high thermal stability and high T_g. Nevertheless, its hydrolyzability and nondurability were the crucial problems when used as high performance polymer in manufacturing process.

Chapter 3 described the syntheses of high performance bio-based PIs which were used in place of the polyamide. However, bio-based PIs were very difficult to prepare since the aromatic diamines could not be made using biosynthesis as they are

generally strongly incompatible with microorganism or plant cells. The bio-based PIs were synthesized by the stepwise thermal imidization of poly(amic acid)s (PAAs) processed at the maximum temperature of 250 °C. PAAs showed high molecular weight and high intrinsic viscosity. In the case of PIs, they showed ultrahigh thermal resistance with T_g over 350 °C, the highest value of all bio-based plastics reported as far as I know. In addition, PI films also possessed properties such as light weight, high tensile strength, high Young's modulus, and high refractive indices.

Not only thermal and mechanical properties, but also transparency and chemical resistance of PIs were studied in **Chapter 4.** PI films which showed high transparency and high refractive indices were suitable to use in optical applications such as fiber optics and micro lens. In addition, these bio-based PIs were also compatibility with cells which can lead to the development of high performance biomedical materials, especially in ophthalmological applications. Durability of the materials is one of the factors required for using in the industry. All PIs showed resistance to light, rain, moisture and bacteria.

The development of high-performance PIs generally show excellent durability but that also they are means less environmentally degradable, which may sometimes induce the negative effects on establishment of green-sustainable society. Hence, the degradability under specific condition is strongly requested. The PIs should potentially be applied as super-engineering plastics that are highly durable under useful lifetime but degradable after use. Moreover, they could help cut the amount of petroleum necessary for producing plastics and reduce the devastating problem of carbon dioxide condensation in the earth's atmosphere which enhances global warming.

ACHIEVEMENTS

Publications:

Major research

1. Suvannasara, P., Tateyama, S., Miyazato, A., Matsumura, K., Shimoda, T., Ito, T., Yamagata, Y., Fujita, T., Takaya, N. & Kaneko, T. Biobased polyimides from 4-aminocinnamic acid photodimer. *Macromolecules, 47,* 1586-1593.
2. Suvannasara, P., Tateyama, S., Miyazato, A., Kaneko, T. Low thermal expansion bio-based polyimide with their degradable property. *In Preparation for Polymer Degradation and Stability*.
3. Tateyama, S., Suvannasara, P., Oka, Y., Kaneko, D., Okajima, M. K., Ito, T., Yamagata, Y., Fujita, T., Takaya, N. & Kaneko, T. Ultra-high performance, degradable bioplastics derived from microbial photodimers. *Submitted to Sciences*.

Minor research

4. Suvannasara, P., Juntapram, K., Praphairaksit, N., Siralertmukul, K. & Muangsin, N. (2013). Mucoadhesive 4-carboxybenzenesulfonamide-chitosan with antibacterial properties. *Carbohydrate Polymers*, *94*, 244-252.
5. Suvannasara, P., Siralertmukul, K. & Muangsin, N. 4-carboxybenzene sulfonamide -chitosan mucoadhesive microsphere for acetazolamide delivery. *International Journal of Biological Macromolecule, 64, 240-246*.
6. Suvannasara, P., Praphairaksit, N., Siralertmukul, K. & Muangsin, N. Synthesis and characterization of sulfanilamide-chitosan as mucoadhesive polymer. *In preparation*.

7. Suvannasara, P., Praphairaksit, N., Siralertmukul, K. & Muangsin, N. Self-assembly of *N*-Trimethyl 4-carboxybenzenesulfonamide-chitosan mucoadhesive nanofibers. *In preparation*.

Conferences:

1. Suvannasara, P., Praphairaksit, N., Siralertmukul, K. & Muangsin, N. Mucoadhesive polymer as a drug delivery system: synthesis and evaluation of chitosan-4-carboxybenzenesulfonamide conjugates. The 11th International Conference on Chitin and Chitosan. The 8th Asia-Pacific Chitin and Chitosan Symposium, Taipei, Taiwan, 6-9 September 2009 *(Oral presentation)*.
2. Suvannasara, P., Praphairaksit, N., Siralertmukul, K. & Muangsin, N. 4-Carboxybenzenesulfonamide-chitosan microsphere for immobilization of carbonic anhydrase inhibitor by electrospray technique. The 7th International Symposium on Advanced Materials in Asia-Pacific and Japan Advanced Institute of Science and Technology (JAIST) International Symposium on Nano Technology 2010, Ishikawa, Japan, 30 September-10 October 2010 *(Poster presentation)*.
3. Suvannasara, P., Miyazato, A., Tateyama, S., & Kaneko, T. Preparation of bio-based polyimides from 4-aminocinnamic acid, 平成23年度北陸地区講演会と研究発表会, Kanazawa University, Ishikawa, Japan, 18 November 2011 *(Poster presentation)*.
4. Suvannasara, P., Miyazato, A., Tateyama, S., & Kaneko, T. Syntheses of bio-based polyimides from cinnamate biochemicals. 3rd International Workshop on Polymer Engineering and Processing and 2nd International Symposium of Highly

Environmental and Recyclable Polymers, Japan Advanced Institute of Science and Technology (JAIST), Ishikawa, Japan, 21 November 2011 *(Oral presentation)*.

5. Suvannasara, P., Miyazato, A., Tateyama, S., & Kaneko, T. Syntheses of bio-based polyimides derived from photodimers of cinnamate biochemicals. Kyoto International Conference Center, Takaragaike, Sakyo-ku, Kyoto, Japan, 29-31 May 2013 *(Oral presentation)*.
6. Suvannasara, P., Miyazato, A., Tateyama, S., Matsumura, K., Shimoda, T., Takaya, N. & Kaneko, T. Preparation of bio-based polyimides from 4-aminocinnamate and their surface properties evaluation as biomaterials. 62nd Symposium for Macromolecule. Kanazawa University, Ishikawa, Japan, 11-13 September 2013 *(Poster presentation)*.
7. Suvannasara, P., Miyazato, A., Tateyama, S., Matsumura, K., Shimoda, T., Takaya, N. & Kaneko, T. High performance bio-based polyimides derived from 4-aminocinnamate as biomaterials. The 4th International Conference on Bio-based Polymers (ICBP2013), Seoul, Korea, 25-28 September 2013 *(Poster presentation)*.
8. Suvannasara, P., Miyazato, A., Tateyama, S., Matsumura, K., Shimoda, T., Takaya, N. & Kaneko, T. High performance bio-based polyimides derived from 4-aminocinnamate as biomaterials. 1st JAIST Poster Challenge, Japan Advanced Institute of Science and Technology (JAIST), Ishikawa, Japan, 12 October 2013 *(Poster presentation)*.
9. Suvannasara, P., Miyazato, A., Tateyama, S., Matsumura, K., Shimoda, T., Takaya, N. & Kaneko, T. Bio-based polyimides derived from photodimers of

cinnamate with their high performance, surface energy, and cell adhesion, IUPAC 9th International Conference on Novel Materials and Synthesis (NMS-IX) & 23rd International Symposium on Fine Chemistry and Functional Polymers (FCFP-XXIII), Shanghai, 17-22 October 2013 *(Poster presentation).*

Awards:

Title: Bio-based polyimides derived from photodimers of cinnamate with their high performance, surface energy, and cell adhesion.

Poster award on IUPAC 9th International Conference on Novel Materials and Synthesis (NMS-IX) & 23rd International Symposium on Fine Chemistry and Functional Polymers (FCFP-XXIII), Shanghai, 17-22 October 2013.

ACKNOWLEDGEMENTS

This study was performed at School of Materials Sciences, Japan Advanced Institute of Science and Technology (JAIST), Japan and was financially supported by Advanced Low Carbon Technology Research and Development Program (JST ALCA, 5100270), Tokyo, Japan.

I would like to express my sincere gratitude to my supervisor, Associate Professor Tatsuo Kaneko of JAIST for his active valuable guidance, helpful suggestions and kindly support during my staying in Japan. All of achievements during my study would not be possible without his creative mind and his enthusiastic guidance.

I also express my specially thank my second supervisor Prof. Kohki Ebitani and my advisor for minor research Prof. Masayuki Yamaguchi in JAIST for their valuable guidance and creative mind in Japan.

I also thank Dr. Akio Miyazato and Research Assistants Professor Seiji Tateyama of JAIST to all appreciate comment and suggestions. They made me improve my scientific skill and made me believe that I can be the good scientist.

I would like to grateful acknowledge Dr. Maiko Okajima for her kindness and concern that made it possible for me to complete my study without any difficulties in JAIST, Associate Professor Kazuaki Matsumura for their good discussion and supported me to do culture cell, Professor Tatsuya Shimoda for good advice and contact angle machine supporting and Prof. Naoki Takaya for support me about biological method and biological product.

I would like to express my appreciation to my referees, Prof. Noriyoshi Matsumi, Prof. Minoru Terano and Prof. Masayuki Yamaguchi of JAIST and Prof.

Masa-aki Kakimoto of Tokyo Institute of Technology for their assistance to complete my thesis.

I would like to thank all of my lab mates, Mr. Kai Kan, Mr. Katsuaki Yasaki, Mr. Wang Siqian, Ms. Nguyen Thi Le Quyen, Ms. Pham Thi Thanh Huyen, Mr. Jin Xin, Mr. Hieu Duc Nquyen, Ms. Kittima Amornwachirabodee, Mr. Asif Mohammad, Mr. Amit Kumar, Mr. Shin Hojoon, Mr. Yuuki Oka, Mr. Masanori Miyasato, Ms. Nupur Tandon, Ms. Rupali Sharma, Mr. Kawamoto Hirotoshi, Mr. Kohei Goto, Mr. Takahiro Noda, Mr. Hiroshi Shimosegawa, Mr. Ryosuke Mishima, Ms. Risa Tsuji, Mr. Motoki Misumi, Mr. Tomohito Shimada, Ms. Ayaka Sano for help me and sharing happy time.

I would like to express my grateful acknowledge to my advisor in Thailand, Associate Professor Nongnuj Muangsin of Faculty of Science, Chulalongkorn University, Thailand for her invaluable guidance, open mind, encouragement during my study in Japan. She made me stronger and stands at this point as well.

I would like to express my gratefulness to my Dual Degree Program corporate between Chulalongkorn University, Thailand and JAIST, Japan for finally supported during my study in Japan.

Finally, I would like to express my heartfelt appreciation to my parents Patpong Suvannnasara and Raweewun Suvannasara and my lovely sister Kochakorn Suvannasara for thoughtful attention and continuous encouragements.

March 2014

JAIST

Phruetchika Suvannasara

REFERENCES

[1] Derraik, Jose G. B. *Mar. Pollut. Bull.* **2002**, *44*, 842–852.

[2] Parrenin, F.; Masson-Demotte, V.; Kohler, P.; Raynaud, D.; Paillard, D.; Schwander, J.; Barbante, C.; Landais, A.; Wegner, A.; Jouzel, J. *Science* **2013**, *339*, 1060-1063.

[3] Stevens, E. S. *Green plastics: An introduction to the new science of biodegradable plastics*, Princeton University Press, Princeton.

[4] Vert, M. *Biomacromolecules* **2005**, *6(2)*, 538-546.

[5] Taniguchi, I.; Kimura, Y. *Biopolymers* **2001**, *3b*, 431.

[6] Saulnier, B.; Ponsart, S.; Coudane, J.; Garreau, H.; Vert, M. *Macromole. Biosci.* **2004**, *4(3)*, 232-237.

[7] Yamamoto, M.; Witt, U.; Skupin, G.; Beimbore, D.; Mueller, R.-J. *Biopolymers* **2002,** *4*, 299-305.

[8] Nagarajan, V.; Singh, M.; Kane, H.; Khalili, M.; Bramucci, M. J. *Polym. Environ.* **2006**, *14*, 281-287.

[9] Pellequer, J. L.; Wager-Smith, K. A.; Kay, S. A.; Getzoff, E. D. *Proc. Natl. Acad. Sci. USA* **1998**, *95*, 5884-5890.

[10] Harris, P. J.; Hartley, R. D. *Nature* **1976,** *259*, 508-510.

[11] Yasaki, K.; Suzuki, T.; Yazawa, K.; Kaneko, D.; Kaneko, T. *J. Polym. Sci.Part A: Polym. Chem.* **2011**, *49*, 1112-1118.

[12] He, J.; Magarvey, N.; Piraee M., Vining, L. C. *Microbiology* **2001**, *147*, 2817-2829.

[13] Mehl, R. A. et al. *J. Am. Chem. Soc.* **2003,** *125*, 935-939.

[14] Yanai K et al. *Nat. Biotechnol.* **2004**, *22*, 848-855.

[15] Sliemandagger, T. A.; Nicholson, W. L. *Appl. Environ. Microbiol.* **2001**, *67(3)*, 1274-1279.

[16] Garcia, J. M.; Garcia, F. C.; Serna, F.; de la Pena, J. *Prog. Polym. Sci.* **2010,** *35*, 623-686.

[17] Overberger, C.; Moore, J. A. *Adv. Polymer. Sci.* **1970**, *7*, 113-150.

[18] Hergenrother, P. M. *High. Perform. Polym*, **2003,** *15*, 3-45.

[19] Lim, J. G.; Gupta, B.S.; George, W. *Prog. Polym. Sci*, **1989**, *14*, 763-809.

[20] Suh, D. H.; Ju, S. Y.; Park, S. H.; Lee, J. W. *J. Macromol. Sci. Pure Appl. Chem.* **2001**, *38*, 751-760.

[21] Morgan, P. W. *Macromolecules* **1977,** *10*, 1381-1390.

[22] Lin, J.; Sherrington, D. C. *Adv. Polym. Sci*. **1994**, *111*, 176-219.

[23] Akamatsu, K.; Ikeda, S., Nawafune, H. *Langmuir* **2003,** *19*, 10366-10371.

[24] Xu, K.; Economy, J. *Macromolecules* **2004**, *37*, 4146-4155.

[25] Zhang, S.; Li, Y.; Yin, D, Wang, X.; Zhao, X.; Shao, Y.; Yang, S. *Eur. Polym. J.* **2005**, *41*, 1097-1107.

[26] Hergenrother, P. M.; Watson, K. A.; Smith, J. G.; Connell, J. W.; Yokota, R. *Polymer* **2002**, *43*, 5077-5093.

[27] Diaham, S.; Locatelli, M. L.; Lebey, T.; Malec, D. *Thin Solid Films* **2011**, *519*, 1851-1859.

[28] Kailani, M. H.; Sung, C. S. P.; Huang, S. J. *Macromolecules* **1992**, *25*, 3751-3757.

[29] Wang, Z. Y., Bender Timothy, P.; Zheng, H. B.; Chen, L. Z. *Polym. Adv. Technol.* **2000**, *11*, 652-657.

[30] Zhou, H. W.; Liu, J. G.; Qian, Z. G.; Zhang, S. Y.; Yang, S. Y. J. *Polym. Sci., Part A: Polym. Chem.* **2001**, *39*, 2404-2413.

[31] Bryce, R. M.; Nguyen, H. T., Nakeeran, P.; Clement, T.; Haugen, C. J. *Thin Solid Films* **2004**, *458*, 233-236.

[32] Chen G.-Q. Chen, M. K. Patel, *Chem. Rev.* **2012**, *112(4)*, 2082-2087.

[33] Kaneko, T.; Suzuki, T.; Wang, S.; Kaneko, D. *Int. J. Chem. Environ. Eng.* **2010**, *1*, 133-135.

[34] Kaneko, T.; Tran, H. T.; Shi, D. J.; Akashi, M. *Nature Mater*. **2006**, *5*, 966-970.

[35] Sheldrick, G. M. *SHELXS97* and *SHELXL97*. University of Göttingen, Germany. **1997**.

[36] Yang, H.; Jia, L.; Wang, Z., Di-Cicco, A.; Levy, D.; Keller, P. *Macromolecules* **2011**, 44, 159-165.

[37] Ronava, I. A.; Bruma, M. *Struct. Chem*. **2010**, *21*, 1013-1020.

[38] Choi, M.-C.; Wakita, J.; Ha, C.-S.; Ando, S. *Macromolecules* **2009**, *42*, 5112-5120.

[39] Mallakpour, S.; Dinari, M. *Ira. Polm. J*. **2010**, *19 (12)*, 983-1004.

[40] Shao, Y.; Li, Y.-F.; Zhao, X.; Wang, X.-L.; Ma, T.; Yang, F.-C. J. *Polym. Sci., Part A: Polym. Chem*. **2006**, *44*, 6836-6846.

[41] Mathews, A. S.; Kim, I.; Ha, C.-S. *Macromol. Res*. **2007**, *15*, 114-128.

[42] Anyalebechi, P. N. "Materials Science and Engineering Laboratory Manual" School of Engineering, Padnos College of Engineering and Computing, Grand Valley State University, January 2005, pp. 59-60, 85.

[43] Reis, R. L.; Cunha, A. M. *J. Mater. Sci. Mater. Med*. **1995**, *6*, 786-792.

[44] Reis, R. L.; Mendes, S. C., Cunha, A. M., Bevis, M. *Polym. Int*. **1997,** *43*, 347-353.

[45] Kumari, A.; Yadav, S. K.; Yadav, S. C. *Colloids Surf., B: Bioterfaces*. **2010,** *7(1)* 1-18.

[46] Jung, J.; Lee, I.-H.; Lee, E., Park, J., Jon S. *Biomacromolecules* **2007**, *8 (11)*, 3401-3407.

[47] Gomes, M. E.; Ribeiro, A. S.; Malafaya, P. B.; Reis, R. L.; Cunha, A. M. *Biomaterials* **2001**, *22*, 883-889.

[48] Swetha, M.; Sahithi, K., Moorthi, A., Srinivasan, N., Ramasamy, K.; Selvamurugan, N. *Int. J. of Biol. Macromol*. **2010**, *47 (1)*, 1-4.

[49] Speidel, M. O. & Uggowitzer, P. J. *Materials in Medicine, vdfHochschulverlag AG an der ETH zurich*, Switzerland, **1998,** pp 191-208.

[50] Ramakrishna, S.; Mayer, J.; Wintermantel, E., Leong, K. W. *Compos. Sci. Technol.* **2001,** *61 (9)*, 1189-1224.

[51] Ishihara, K.; Fukumoto, K.; Iwasaki, Y., Nakabayashi, N. *Biomaterials* **1999**, *20*, 1545-1551.

[52] Ulery, B. D.; Nair, L. S.; Laurencin, C. T. *J. Polym. Sci. B. Polym. Phys*. **2011**, *49 (12)*, 832-864.

[53] Marques, A. P.; Reis, R. L.; Hunt, J. A. *Biomaterials* **2002**, *23*, 1471-1478.

[54] Fukuzaki, N.; Higashihara, T.; Ando, S.; Ueda, M. *Macromolecules* **2010**, *43*, 1836-1843.

[55] Amssian, H. L. *Acta. Orthopedica, Scand.* **1999**, *70 (6)*, 578.

[56] Amstutz, H. C. *J. Biomeducal Material Res.* **1968**, *3*, 547.

[57] Suzuki, H.; Ohnishi, Y.; Furusho, Y.; Sakuda, S.; Horinouchi, S. *J. Biol. Chem.* **2006**, *281*, 36944–36951.

[58] Noguchi, A.; Kitamura, T.; Onaka, H.; Horinouchi, S.; Ohnishi, Y. *Nat. Chem.*

Biol. **2010**, *6*, 641–643.

[59] Johnson, O. H.; Green, D. E.; Pauli, R. *J. Biol. Chem.* **1994**, *153*, 37–47.

[60] Yokota, T.; Terai, T.; Kobayashi, T.; Meguro, T.; Iwaki, M. *Surf. Coat. Technol*. **2007**, *201*, 8048-8051.

[61] Rizzarelli, P.; Puglisi, C.; Montaudo, G. *Polym*. *Degrad*. *Stab*. **2004**, *85*, 855-863.

[62] Lu, Y.; Hu Z.; Wang, Y.; Fang, Q. X. *J. Appl. Polym. Sci.* **2012**, 125(2), 1371-1376.

[63] Hasegawa, M.; Horie, K. *Prog. Polym. Sci.* **2001**, *26*, 259-335.

[64] Inagaki, N.; Tasaka, S.; Hibi, K. J. *Adhesion. Sci. Technol*. **1994**, *8*, 395.

[65] Harnett, E. M.; Alderman, J.; Wood, T. *Colloids Surf., B: Bioterfaces*. **2007,** 90-97.

[66] Ball, M. D.; Prendergast U.; O' Connell, C.; Sherlock, R. *Macromol*. *Res.* **2007**, *82(2)*, 130-134.

APPENDIX

Table A1 Atomic coordinates ($\times 10^4$) and equivalent isotropic displacement parameters ($A^2 \times 10^3$) for 4,4'-diamino-α-truxillic acid dihydrochloride, $^aU_{(eq)}$ is defined as one third of the trace of the orthogonalized U_{ij} tensor.

	x	y	z	U_{iso}*/U_{eq}
O1	0.1511 (3)	0.6645 (3)	0.67431 (16)	0.0551(6)
H1	0.1584	0.7040	0.7447	0.083*
O2	0.5582 (4)	0.8184 (3)	0.71549 (19)	0.0696 (7)
N1	0.6859 (4)	0.8240 (3)	0.0555 (2)	0.0527 (7)
H1A	0.7344	0.9498	0.0700	0.079*
H1B	0.5368	0.7748	0.0109	0.079*
H1C	0.7952	0.7765	0.0191	0.079*
C1	0.6716 (5)	0.7762 (4)	0.1653 (2)	0.0411 (7)
C2	0.8775 (5)	0.8445 (4)	0.2501 (3)	0.0488 (7)
H2	1.0261	0.9217	0.2387	0.059*
C3	0.8616 (5)	0.7975 (4)	0.3527 (2)	0.0455 (7)
H3	1.0011	0.8438	0.4104	0.055*
C4	0.6404 (5)	0.6818 (4)	0.3714 (2)	0.0396 (7)
C5	0.6299 (5)	0.6233 (4)	0.4812 (2)	0.0413 (7)
H5	0.7651	0.7122	0.5424	0.050*
C6	0.3792 (5)	0.5884 (4)	0.5281 (2)	0.0412 (7)
H6	0.2457	0.5925	0.4728	0.049*
C7	0.3809 (5)	0.7070 (4)	0.6480 (2)	0.0450 (7)

	x	y	z	U_{iso}*/U_{eq}
C8	0.4494 (5)	0.6617 (4)	0.1803 (2)	0.0470 (7)
H8	0.3105	0.6165	0.1224	0.056*
C9	0.43734 (12)	0.61550 (11)	0.28348 (6)	0.0485 (8)
H9	0.2884	0.5376	0.2940	0.058*
C11	0.13099 (12)	0.74325 (11)	0.93291 (6)	0.0529 (3)

Table A2 Selected bond lengths (A°) and angle (°) for 4,4'-diamino-α-truxillic acid dihydrochloride. Symmetry transformations used to generate equivalent atoms: -x+1, -y+1,-z+1

Bonds	Length (A°)	Bonds	Angle (°)
O1–C7	1.338 (3)	C7–O1–H1	109.5
O1–H1	0.8200	O2–O2–C7	0 (10)
O2–O2	0.000 (7)	C1–N1–H1A	109.5
O2–C7	1.200 (3)	C1–N1–H1B	109.5
N1–C1	1.470 (3)	H1A–N1–H1B	109.5
N1–H1A	0.8900	C1–N1–H1C	109.5
N1–H1B	0.8900	H1A–N1–H1C	109.5
N1–H1C	0.8900	H1B–N1–H1C	109.5
C1–C2	1.371 (4)	C2–C1–C8	121.4 (2)
C1–C8	1.379 (3)	C2–C1–N1	119.8 (2)
C2–C3	1.383 (4)	C8–C1–N1	118.8 (2)
C2–H2	0.9300	C1–C2–C3	119.2 (2)
C3–C4	1.396 (3)	C1–C2–H2	120.4

Bonds	Length (A°)	Bonds	Angle (A°)
C3–H3	0.9300	C3–C2–H2	120.4
C4–C9	1.383 (3)	C2–C3–C4	121.3 (2)
C4–C5	1.508 (3)	C2–C3–H3	119.4
C5–C6	1.552 (4)	C4–C3–H3	119.4
C5–C6^{i}	1.580 (4)	C9–C4–C3	117.6 (2)
C5–H5	0.9800	C9–C4–C5	121.71 (19)
C6–C7	1.497 (4)	C3–C4–C5	120.6 (2)
C6–C5^{i}	1.580 (4)	C4–C5–C6	117.9 (2)
C6–H6	0.9800	C4–C5–C6^{i}	117.4 (2)
C7–O2	1.200 (3)	C6–C5–C6^{i}	89.20 (19)
C8–C9	1.385 (3)	C4–C5–H5	110.3
C8–H8	0.9300	C6–C5–H5	110.3
C9–H9	0.9300	C6^{i}–C5–H6	110.3
C11–C11	0.0000 (14)	C7–C6–C5	117.0 (2)
		C7–C6–C5^{i}	114.3 (2)
		C5–C6–C5^{i}	90.80 (19)
		C7–C6–H6	111.1
		C5–C6–H6	111.1
		C5^{i}–C6–H6	111.1
		O2–C7–O2	0.0 (2)
		O2–C7–O1	122.9 (3)
		O2–C7–O1	122.9 (3)
		O2–C7–C6	127.2 (3)
		O2–C7–C6	127.2 (3)
		O1–C7–C6	109.8 (2)

Bonds	Length (A°)	Bonds	Angle (A°)
		C1–C8–C9	118.6 (2)
		C1–C8–H8	120.7
		C9–C8–H8	120.7
		C4–C9–C8	121.95 (16)
		C4–C9–H9	119.0
		C8–C9–H9	119.0